Fraunhofer Institut
Techno- und
Wirtschaftsmathematik

S. Panda, R. Wegener, N. Marheineke

Slender Body Theory for the Dynamics of Curved Viscous Fibers

Berichte des Fraunhofer ITWM, Nr. 86 (2006)

ISSN 1434-9973

Bericht 86 (2006)

Die Veröffentlichungen in der Berichtsreihe des Fraunhofer ITWM können bezogen werden über:

Fraunhofer-Institut für Techno- und
Wirtschaftsmathematik ITWM
Fraunhofer-Platz 1

67663 Kaiserslautern
Germany

Telefon: +49 (0) 6 31/3 16 00-0
Telefax: +49 (0) 6 31/3 16 00-10 99
E-Mail: info@itwm.fraunhofer.de
Internet: www.itwm.fraunhofer.de

Vorwort

Das Tätigkeitsfeld des Fraunhofer Instituts für Techno- und Wirtschaftsmathematik ITWM umfasst anwendungsnahe Grundlagenforschung, angewandte Forschung sowie Beratung und kundenspezifische Lösungen auf allen Gebieten, die für Techno- und Wirtschaftsmathematik bedeutsam sind.

In der Reihe »Berichte des Fraunhofer ITWM« soll die Arbeit des Instituts kontinuierlich einer interessierten Öffentlichkeit in Industrie, Wirtschaft und Wissenschaft vorgestellt werden. Durch die enge Verzahnung mit dem Fachbereich Mathematik der Universität Kaiserslautern sowie durch zahlreiche Kooperationen mit internationalen Institutionen und Hochschulen in den Bereichen Ausbildung und Forschung ist ein großes Potenzial für Forschungsberichte vorhanden. In die Berichtreihe sollen sowohl hervorragende Diplom- und Projektarbeiten und Dissertationen als auch Forschungsberichte der Institutsmitarbeiter und Institutsgäste zu aktuellen Fragen der Techno- und Wirtschaftsmathematik aufgenommen werden.

Darüberhinaus bietet die Reihe ein Forum für die Berichterstattung über die zahlreichen Kooperationsprojekte des Instituts mit Partnern aus Industrie und Wirtschaft.

Berichterstattung heißt hier Dokumentation darüber, wie aktuelle Ergebnisse aus mathematischer Forschungs- und Entwicklungsarbeit in industrielle Anwendungen und Softwareprodukte transferiert werden, und wie umgekehrt Probleme der Praxis neue interessante mathematische Fragestellungen generieren.

Prof. Dr. Dieter Prätzel-Wolters
Institutsleiter

Kaiserslautern, im Juni 2001

Slender Body Theory for the Dynamics of Curved Viscous Fibers

Satyananda Panda[1], Raimund Wegener[2], Nicole Marheineke[3]

[1,2] Fraunhofer-Institut für Techno- und Wirtschaftsmathematik (ITWM)
Fraunhofer-Platz 1, D-67663 Kaiserslautern
panda@itwm.fhg.de, wegener@itwm.fhg.de

[3] Technische Universität Kaiserslautern
Fachbereich Mathematik
Postfach 3049, D-67653 Kaiserslautern
nicole@mathematik.uni-kl.de

March 1, 2006

Abstract

The paper at hand presents a slender body theory for the dynamics of a curved inertial viscous Newtonian fiber. Neglecting surface tension and temperature dependence, the fiber flow is modeled as a three-dimensional free boundary value problem via instationary incompressible Navier-Stokes equations. From regular asymptotic expansions in powers of the slenderness parameter leading-order balance laws for mass (cross-section) and momentum are derived that combine the unrestricted motion of the fiber center-line with the inner viscous transport. The physically reasonable form of the one-dimensional fiber model results thereby from the introduction of the intrinsic velocity that characterizes the convective terms.

Keywords: Curved viscous fibers; Fluid dynamics; Navier-Stokes equations; Free boundary value problem; Asymptotic expansions; Slender body theory

AMS Classification: 41A60, 76D05, 30E25

1 Introduction

In the production process of glass wool, hot molten glass is pressed through narrow nozzles of a rotating cylindrical drum by the acting centrifugal forces. Thereby, thin fibers are formed that break into filaments due to the surrounding air flow and fall down onto a conveyor belt.

Focusing on the spinning process in this paper, we deal with a single slender curved viscous fiber in motion. Neglecting temperature dependence and surface tension, the fiber medium is modeled as incompressible Newtonian fluid and the fiber forming as three-dimensional free boundary value problem (BVP) in terms of incompressible Navier-Stokes equations with inflow boundary and stress-free surface conditions. In spite of the made assumptions the problem is still very complex and difficult to handle. But, the slender fiber geometry enables its asymptotic consideration and simplification to an one-dimensional fiber model for mass and momentum.

In the context of molten glass draw-down, glass-fiber tapering and polymer-fiber production such a model reduction based on slender body theory is a well-known and appreciated tool and still subject of research. Historically, one-dimensional fiber models have been derived from the assumption of purely extensional flow in combination with the cross-sectional averaging of the balance laws, see references in [6] and [7]. The work of Dewynne et al [6] has been the first systematic derivation approach. It has used regular asymptotic expansions for the simplification of stationary Stokes flow with instationary free surface. Thereby, the fiber center-line has been considered as nearly straight. This paper has undoubtedly formed the basis for

several subsequent studies. Howell [8] has extended this work on a curved, dynamic center-line. In addition, an asymptotic fiber model for instationary Navier-Stokes flow with dynamic but nearly straight center-line has been deduced in [5] excluding and respectively in [3] including surface tension. The restriction on nearly straight fibers enables the asymptotic analysis in Cartesian coordinates.

In our application in contrast, curvature caused by the acting rotational forces plays a crucial role. For such a flow a quite heuristic approach under averaging and stationary assumptions has been stated in [4]. The demand on our paper is the systematic derivation of an asymptotic model for the fiber dynamics without any restrictions on the center-line shape and motion nor on the inner viscous flow. This aim requires the formulation of Navier-Stokes equations in time-dependent curvilinear coordinates. For the asymptotic analysis, we distinguish between the transporting intrinsic velocity and the transported momentum. The splitting and in particular the separate handling of the velocities result in a physically reasonable one-dimensional fiber model for the evolution of mass (cross-sections) and momentum. Thereby, the total velocity consists of the dynamics of the center-line and the intrinsic velocity in tangential direction.

Stating the three-dimensional free BVP for the spinning of a slender curved inertial viscous fiber in Sec 2, the slenderness parameter ϵ is identified as ratio between the radius of the nozzle (inflow boundary) and the typical fiber length. In Sec 3 a general coordinate transformation is introduced that distinguishes between the intrinsic and the transported velocity. The general concept is then specified for scaled curvilinear coordinates that are appropriately adapted to the fiber geometry. In these coordinates the inflow conditions become independent of the slenderness parameter, instead ϵ occurs explicitely in the balance laws. Their asymptotic analysis in Sec 4 follows the spirit of [6] by using the standard expansion techniques in powers of the slenderness parameter for the model reduction. The final one-dimensional fiber model presented in Sec 5 can be understood as generalization of the existing models to the unrestricted dynamic description of a curved viscous fiber.

2 Free Boundary Value Problem

The spinning of a curved viscous fiber is modeled as a three-dimensional free BVP for a Newtonian fluid, in particular it is described in terms of the incompressible Navier-Stokes equations with free surface and inflow boundary conditions. The underlying equations are non-dimensionalized by help of the given constant fluid density ρ, the mean velocity at the nozzle V as well as a fiber length ℓ that is typical in the spinning process. Thus, the process is characterized by the dimensionless Reynolds number $\mathrm{Re} = \rho V \ell / \mu$ with dynamic viscosity μ.

The process is initialized with an empty flow domain at time zero, note that $t \in \mathbb{R}^+$ in the course of this paper. Let the domain of interest at time t be denoted by $\Omega(t) \subset \mathbb{R}^3$ and its boundary by $\partial\Omega(t) = \Gamma_{fr}(t) \cup \Gamma_{in}$ with $\Gamma_{fr}(t) \cap \Gamma_{in} = \emptyset$. Here, $\Gamma_{fr}(t)$ and Γ_{in} prescribe the time-dependent free surface and the time-independent planar inflow boundary (nozzle), respectively. Then, the model for the BVP reads

Balance laws, $\mathbf{r} \in \Omega(t)$

$$\nabla \cdot \mathbf{v}(\mathbf{r},t) = 0$$
$$\partial_t \mathbf{v}(\mathbf{r},t) + \nabla \cdot (\mathbf{v} \otimes \mathbf{v})(\mathbf{r},t) = \nabla \cdot \mathbf{S}^T(\mathbf{r},t) + \mathbf{f}(\mathbf{r},t)$$

Constitutive law

$$\mathbf{S} = -p\,\mathbf{I} + \frac{1}{\mathrm{Re}}(\nabla\mathbf{v} + (\nabla\mathbf{v})^T)$$

Kinematic and dynamic boundary conditions, $\mathbf{r} \in \Gamma_{fr}(t)$

$$(\mathbf{v} \cdot \mathbf{n})(\mathbf{r},t) = w(\mathbf{r},t), \qquad (\mathbf{S} \cdot \mathbf{n})(\mathbf{r},t) = \mathbf{0}$$

Inflow boundary condition, $\mathbf{r} \in \Gamma_{in}$

$$\mathbf{v}(\mathbf{r},t) = \mathbf{v}_{in}(\mathbf{r})$$

Initial condition

$$\Omega(0) = \emptyset$$

Apart from the unknown field variables for velocity $\mathbf{v}$ and pressure p, the stated boundary value problem determines the geometry of the flow domain that is specified by the unit outer normal vectors $\mathbf{n}$ and the scalar speed w of the free surface $\Gamma_{fr}(t)$. By choosing homogeneous dynamic boundary conditions for the stress tensor $\mathbf{S}$ the effects of surface tension are neglected, moreover p is incorporated as the hydrodynamic pressure being relative with respect to the constant atmospheric one. The appropriate choice of body forces $\mathbf{f}$ completes the model. Gravitational and rotational forces are considered in Sec 5.

A fiber in a spinning process is in general long and thin, since the radius of the nozzle is comparably small to the length of the fiber. Thus, a suitable slenderness parameter ϵ is given by

$$| \Gamma_{in} |^{1/2} = \epsilon \ll 1 \tag{1}$$

where $| \Gamma_{in} | = \int_{\Gamma_{in}} \mathrm{d}\mathcal{A}$ is the measure of the cross-sectional area of the nozzle Γ_{in}. Due to the taken typical velocity V, the dimensionless inflow velocity profile $\mathbf{v}_{in}$ at the nozzle satisfies

$$\int\limits_{\Gamma_{in}} \mathbf{v}_{in} \cdot \boldsymbol{\tau}_{\mathbf{0}} \, \mathrm{d}\mathcal{A} = \int\limits_{\Gamma_{in}} \mathrm{d}\mathcal{A} = \epsilon^2 \tag{2}$$

where $\boldsymbol{\tau}_{\mathbf{0}}$ denotes the inner normal vector of the inflow boundary. In this paper, the stated free BVP is asymptotically analyzed with respect to ϵ in the sense of slender body theory. The resulting one-dimensional fiber model is thereby discussed in view of the consequences coming from the discrepancy between the slenderness assumption and the initial condition.

3 Coordinate Transformations

For the asymptotical reduction of the free BVP it is essential to formulate the problem in appropriate fiber coordinates. For this purpose, we firstly transform the free BVP into general coordinates that are then specified as scaled curvilinear. These coordinates can be understood as generalization of cylindrical ones along an arbitrary curve. Scaling leads to inflow conditions being independent of the slenderness parameter ϵ. In terms of these coordinates with the fiber center-line as reference curve the problem is embedded into a family with respect to ϵ.

3.1 General Coordinates

Definition 1 (Time-dependent General Coordinate Transformation)
A function $\breve{\mathbf{r}}$ *defined by* $\breve{\mathbf{r}}(\cdot, t)\colon \hat{\Omega}(t) \subset \mathbb{R}^3 \mapsto \Omega(t) \subset \mathbb{R}^3$ *for* $t \in \mathbb{R}^+$ *is called time-dependent general coordinate transformation if* $\breve{\mathbf{r}} \in \mathcal{C}^2$ *and if its restrictions* $\breve{\mathbf{r}}(\cdot, t)$ *are bijective.*

Notation 2 (Characteristic Quantities)
For a given time-dependent coordinate transformation $\breve{\mathbf{r}}$ *we introduce the following notations:*

- *Inverse mapping* $\breve{\mathbf{r}}(\breve{\mathbf{x}}(\mathbf{r}, t), t) = \mathbf{r}$ *and* $\breve{\mathbf{x}}(\breve{\mathbf{r}}(\mathbf{x}, t), t) = \mathbf{x}$
- *Coordinate transformation matrix* $\mathbf{F}(\mathbf{x}, t) = \nabla_{\mathbf{x}} \breve{\mathbf{r}}(\mathbf{x}, t)$
- *Functional determinant* $J(\mathbf{x}, t) = \det(\mathbf{F}(\mathbf{x}, t))$
- *Inverse matrix* $\mathbf{G}(\mathbf{x}, t) = \mathbf{F}^{-1}(\mathbf{x}, t) = \nabla_{\mathbf{r}} \breve{\mathbf{x}}(\breve{\mathbf{r}}(\mathbf{x}, t), t)$
- *Coordinate velocity* $\tilde{\mathbf{q}}(\mathbf{x}, t) = \partial_t \breve{\mathbf{r}}(\mathbf{x}, t)$ *and* $\mathbf{q}(\mathbf{r}, t) = \tilde{\mathbf{q}}(\breve{\mathbf{x}}(\mathbf{r}, t), t)$

According to Def 1 the function $\breve{\mathbf{r}}$ maps chosen time-dependent coordinates $\mathbf{x}$ onto a spatial point $\mathbf{r}$, whereas $\breve{\mathbf{x}}$ maps any point onto its coordinates. Consequently, scalar, vector and tensor fields can be defined in spatial points or general coordinates. As already applied above for the coordinate velocity, we use the following general convention for any arbitrary function f

$$\tilde{f}(\mathbf{x}, t) = f(\breve{\mathbf{r}}(\mathbf{x}, t), t) \quad \text{and} \quad f(\mathbf{r}, t) = \tilde{f}(\breve{\mathbf{x}}(\mathbf{r}, t), t).$$

Furthermore, the handling of the observables in the free BVP requires transformations that keep the physical and geometrical properties.

Definition 3 (Transformation of Observables)
For the observables of the free BVP the following transformed fields in general coordinates are introduced

- *Mass density* $\quad \hat{\rho}(\mathbf{x},t) = J(\mathbf{x},t)$
- *Stress tensor* $\quad \hat{\mathbf{S}}(\mathbf{x},t) = J(\mathbf{x},t)\,\tilde{\mathbf{S}}(\mathbf{x},t)\cdot\mathbf{G}(\mathbf{x},t)$
- *Intrinsic velocity* $\quad \hat{\mathbf{v}}(\mathbf{x},t) = (\tilde{\mathbf{v}}(\mathbf{x},t) - \tilde{\mathbf{q}}(\mathbf{x},t))\cdot\mathbf{G}(\mathbf{x},t)$
- *Normal vectors* $\quad \hat{\mathbf{n}}(\mathbf{x},t) = \dfrac{\mathbf{F}\cdot\tilde{\mathbf{n}}}{\|\mathbf{F}\cdot\tilde{\mathbf{n}}\|}(\mathbf{x},t)$
- *Surface speed* $\quad \hat{w}(\mathbf{x},t) = \dfrac{(\tilde{w} - \tilde{\mathbf{q}}\cdot\tilde{\mathbf{n}})}{\|\mathbf{F}\cdot\tilde{\mathbf{n}}\|}(\mathbf{x},t)$

The definition of mass ensures that the volume integrals in spatial and general coordinates coincide, e.g. $\int_{\mathcal{B}}\hat{\rho}(\mathbf{x},t)\,\mathrm{d}\mathbf{x} = \int_{\check{\mathbf{r}}(\mathcal{B},t)}\mathrm{d}\mathbf{r}$. Analogously, the definition of stress keeps surface integrals, i.e. traction forces, $\int_{\mathcal{S}}(\hat{\mathbf{S}}\cdot\hat{\mathbf{n}})(\mathbf{x},t)\,\mathrm{d}\mathcal{A} = \int_{\check{\mathbf{r}}(\mathcal{S},t)}(\hat{\mathbf{S}}\cdot\hat{\mathbf{n}})(\mathbf{x},t)\,\mathrm{d}\mathcal{A}$, cf. [1]. Following the concepts of differential geometry, velocities are tangential vectors on time-parameterized curves. Considering corresponding curves in spatial and general coordinates leads directly to the stated transformation rule. As for normal vectors and surface speed, take a moving surface $H(\mathbf{r},t)=0$ in space, then $\mathbf{n}(\mathbf{r},t) = (\nabla_{\mathbf{r}}H/\|\nabla_{\mathbf{r}}H\|)(\mathbf{r},t)$ and $w(\mathbf{r},t) = -(\partial_t H/\|\,\nabla_{\mathbf{r}}H\,\|)(\mathbf{r},t)$. The given definitions provide the analogous relation for $\hat{\mathbf{n}}$ and $\hat{w}$ with respect to $\tilde{H}$.

Theorem 4 (BVP in General Coordinates)
The governing equations of the free BVP in general coordinates read
Balance laws, $\mathbf{x}\in\hat{\Omega}(t)$

$$\partial_t J(\mathbf{x},t) + \nabla_{\mathbf{x}}\cdot(J\hat{\mathbf{v}})(\mathbf{x},t) = 0$$
$$\partial_t(J\tilde{\mathbf{v}})(\mathbf{x},t) + \nabla_{\mathbf{x}}\cdot(\hat{\mathbf{v}}\otimes J\tilde{\mathbf{v}})(\mathbf{x},t) = \nabla_{\mathbf{x}}\cdot\hat{\mathbf{S}}^T(\mathbf{x},t) + (J\tilde{\mathbf{f}})(\mathbf{x},t)$$

Coupling condition

$$\hat{\mathbf{v}} = (\tilde{\mathbf{v}} - \tilde{\mathbf{q}})\cdot\mathbf{G}$$

Constitutive law

$$\hat{\mathbf{S}} = J\left(-\tilde{p}\,\mathbf{I} + \frac{1}{\mathrm{Re}}\left((\mathbf{G}\cdot\nabla\tilde{\mathbf{v}}) + (\mathbf{G}\cdot\nabla\tilde{\mathbf{v}})^T\right)\right)\cdot\mathbf{G}$$

Kinematic and dynamic boundary conditions, $\mathbf{x}\in\hat{\Gamma}_{fr}(t)$

$$(\hat{\mathbf{v}}\cdot\hat{\mathbf{n}})(\mathbf{x},t) = \hat{w}(\mathbf{x},t), \qquad (\hat{\mathbf{S}}\cdot\hat{\mathbf{n}})(\mathbf{x},t) = \mathbf{0}$$

Inflow boundary condition, $\mathbf{x}\in\hat{\Gamma}_{in}$

$$\tilde{\mathbf{v}}(\mathbf{x},t) = \tilde{\mathbf{v}}_{in}(\mathbf{x})$$

Initial condition

$$\hat{\Omega}(0) = \emptyset$$

Proof: Since the physical and geometrical properties are conserved under the transformation, the underlying balance laws are analogously valid for the general coordinates. Under the application of the chain rule a formal proof can be formulated on the basis of the fundamental relations

$$\partial_t J = J\,\nabla_{\mathbf{r}}\cdot\mathbf{q}|_{\mathbf{r}=\check{\mathbf{r}}(\mathbf{x},t)}, \qquad \nabla_{\mathbf{x}}\cdot(J\mathbf{G}^T) = \mathbf{0}.$$

Both are direct consequences of the rule concerning the Frechet derivative of determinants, i.e. $\partial_{\mathbf{A}}\det(\mathbf{A})(\mathbf{B}) = \det(\mathbf{A})\,\mathrm{tr}(\mathbf{A}^{-1}\cdot\mathbf{B})$, cf. [1].

In Th 4 the intrinsic velocity $\hat{\mathbf{v}}(\mathbf{x},t)$ describes the convection/transport of the unknowns in the balance laws in general coordinates, whereas the velocity $\tilde{\mathbf{v}}(\mathbf{x},t) = \mathbf{v}(\check{\mathbf{r}}(\mathbf{x},t),t)$ is associated with the original momentum, i.e. the transported quantity. Their relation is expressed in the coupling condition.

The special case when the coordinate transformation is given by $\partial_t\check{\mathbf{r}} = \tilde{\mathbf{v}}$ with $\check{\mathbf{r}}(\mathbf{x},0) = \mathbf{x}$ yields $\tilde{\mathbf{q}} = \tilde{\mathbf{v}}$ and hence $\hat{\mathbf{v}} = \mathbf{0}$. Here, the general coordinates can be interpreted as Lagrangian coordinates.

3.2 Scaled Curvilinear Coordinates

Let $\boldsymbol{\gamma}(s,t)$ be a three-dimensional time-dependent curve in the domain $\Omega(t) \subset \mathbb{R}^3$ parameterized with respect to the arc-length $s \in \mathbb{R}_0^+$. Assuming sufficient regularity of $\boldsymbol{\gamma}$, curvature $\kappa = \| \partial_{ss}\boldsymbol{\gamma} \|$, $\kappa \neq 0$ and torsion $\lambda = \partial_s\boldsymbol{\gamma} \cdot (\partial_{ss}\boldsymbol{\gamma} \times \partial_{sss}\boldsymbol{\gamma})/\kappa^2$ are well-defined. The tangent, normal and binormal vectors with respect to $\boldsymbol{\gamma}$ are

$$\boldsymbol{\tau} = \partial_s\boldsymbol{\gamma}, \qquad \boldsymbol{\eta} = \frac{1}{\kappa}\partial_{ss}\boldsymbol{\gamma}, \qquad \mathbf{b} = \boldsymbol{\tau} \times \boldsymbol{\eta}.$$

They are related according to the Serret-Frenet formulae

$$\partial_s\boldsymbol{\tau} = \kappa\boldsymbol{\eta}, \qquad \partial_s\boldsymbol{\eta} = -\kappa\boldsymbol{\tau} + \lambda\mathbf{b}, \qquad \partial_s\mathbf{b} = -\lambda\boldsymbol{\eta}.$$

Following [2] the normal and binormal vector are replaced by

$$\boldsymbol{\eta_1} = \cos(\phi)\boldsymbol{\eta} - \sin(\phi)\mathbf{b}, \qquad \boldsymbol{\eta_2} = \sin(\phi)\boldsymbol{\eta} + \cos(\phi)\mathbf{b} \tag{3}$$

with the torsion angle $\phi(s,t) = \int_0^s \lambda(\sigma,t)\,\mathrm{d}\sigma$. Then, the Serret-Frenet formulae can be rewritten as

$$\partial_s\boldsymbol{\tau} = (\partial_\alpha h)\boldsymbol{\eta}_\alpha, \qquad \partial_s\boldsymbol{\eta}_\alpha = -(\partial_\alpha h)\boldsymbol{\tau},\ \alpha = 1,2 \tag{4}$$

where

$$h(\mathbf{x},t) = x_1\kappa\cos(\phi) + x_2\kappa\sin(\phi).$$

Note that the generalized Einstein summation convention is applied in this paper. Thereby, Latin indices have values out of the set $\{1,2,3\}$, Greek indices out of $\{1,2\}$.

Definition 5 (Scaled Curvilinear Coordinate Transformation)
For a given arc-length parameterized and smooth curve $\boldsymbol{\gamma}$ and a fixed parameter $\epsilon \in \mathbb{R}^+$ the special choice of a time-dependent general coordinate transformation

$$\check{\mathbf{r}}(\mathbf{x},t) = \boldsymbol{\gamma}(s,t) + \epsilon\, x_1\boldsymbol{\eta_1}(s,t) + \epsilon\, x_2\boldsymbol{\eta_2}(s,t) \quad \textit{with} \quad s = x_3$$

is called scaled curvilinear coordinate transformation, if $\check{\mathbf{r}}(\cdot,t)$ is bijective for $t \in \mathbb{R}^+$.

Computation 6 (Characteristic Quantities)
Using the canonical basis $\mathbf{e_i}, i = 1,2,3$ in $\mathbb{R}^3$, the characteristic quantities of a scaled curvilinear coordinate transformation are determined as

- *Coordinate transformation matrix* $\quad \mathbf{F} = \mathbf{e_i} \otimes \mathbf{f_i}$
  $\mathbf{f_1} = \epsilon\,\boldsymbol{\eta_1}, \quad \mathbf{f_2} = \epsilon\,\boldsymbol{\eta_2}, \quad \mathbf{f_3} = (1-\epsilon h)\,\boldsymbol{\tau}$
- *Functional determinant* $\quad J = \epsilon^2(1-\epsilon h)$
- *Inverse matrix* $\quad \mathbf{G} = \mathbf{g_i} \otimes \mathbf{e_i}$
  $\mathbf{g_1} = \frac{1}{\epsilon}\boldsymbol{\eta_1}, \quad \mathbf{g_2} = \frac{1}{\epsilon}\boldsymbol{\eta_2}, \quad \mathbf{g_3} = \frac{1}{(1-\epsilon h)}\boldsymbol{\tau}$
- *Coordinate velocity* $\quad \tilde{\mathbf{q}} = \partial_t\boldsymbol{\gamma} + \epsilon\, x_\alpha\partial_t\boldsymbol{\eta}_\alpha$

The basic idea of the computation is the decomposition of $\mathbf{F} = \nabla_{\mathbf{x}}\check{\mathbf{r}}$ in rows $\mathbf{f_i} = \partial_i\check{\mathbf{r}}$. The remaining results can be directly concluded from the definition of the coordinate transformation and the properties of the curve (4). The convenient representation of the characteristic quantities in terms of the basis vectors $\boldsymbol{\eta_1}$, $\boldsymbol{\eta_2}$ and $\boldsymbol{\tau}$ motivates the introduced transformation in Eq (3).

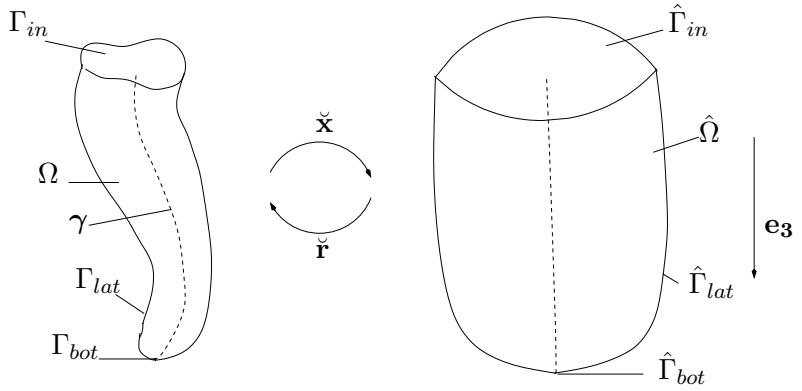

Figure 1: Fiber domain in spatial (left) and scaled curvilinear coordinates (right)

Theorem 7 (Stress Tensor in Scaled Curvilinear Coordinates)
The Newtonian stress tensor of the free BVP in scaled curvilinear coordinates reads

$$\begin{aligned}\hat{\mathbf{S}} = &-\tilde{p}\,\Big(\epsilon(1-\epsilon h)\,(\boldsymbol{\eta}_\alpha \otimes \mathbf{e}_\alpha) + \epsilon^2\,(\boldsymbol{\tau}\otimes\mathbf{e_3})\Big)\\
&+\frac{1}{\mathrm{Re}}\,\Big(\epsilon(1-\epsilon h)\,(\partial_\alpha(\hat{\mathbf{v}}\cdot\mathbf{e}_\beta)+\partial_\beta(\hat{\mathbf{v}}\cdot\mathbf{e}_\alpha))\;(\boldsymbol{\eta}_\alpha\otimes\mathbf{e}_\beta)\\
&\quad+(\epsilon(1-\epsilon h)\partial_\alpha(\hat{\mathbf{v}}\cdot\mathbf{e_3})+\frac{\epsilon^3}{(1-\epsilon h)}\partial_s(\hat{\mathbf{v}}\cdot\mathbf{e}_\alpha))\;(\boldsymbol{\eta}_\alpha\otimes\mathbf{e_3})\\
&\quad+\big(\epsilon^2\partial_s(\hat{\mathbf{v}}\cdot\mathbf{e}_\alpha)+(1-\epsilon h)^2\partial_\alpha(\hat{\mathbf{v}}\cdot\mathbf{e_3})\big)\;(\boldsymbol{\tau}\otimes\mathbf{e}_\alpha)\\
&\quad+(2\,\epsilon^2\partial_s(\hat{\mathbf{v}}\cdot\mathbf{e_3})-\frac{2\epsilon^3}{(1-\epsilon h)}\,(\partial_t h+(\hat{\mathbf{v}}\cdot\mathbf{e}_\alpha)\partial_\alpha h+(\hat{\mathbf{v}}\cdot\mathbf{e_3})\partial_s h))\;(\boldsymbol{\tau}\otimes\mathbf{e_3})\Big)\end{aligned}$$

Proof: Starting from the stress tensor in general coordinates (constitutive law in Th 4), the velocity $\tilde{\mathbf{v}}$ is replaced by $\hat{\mathbf{v}}$ according to the reformulated coupling condition, i.e. $\tilde{\mathbf{v}} = \hat{\mathbf{v}}\cdot\mathbf{F}+\tilde{\mathbf{q}}$. This leads to

$$\begin{aligned}\hat{\mathbf{S}} = J\Big(&-\tilde{p}\,\mathbf{I}+\frac{1}{\mathrm{Re}}\Big((\mathbf{G}\cdot\nabla\hat{\mathbf{v}}\cdot\mathbf{F})+(\mathbf{G}\cdot\nabla\hat{\mathbf{v}}\cdot\mathbf{F})^T+(\mathbf{G}\cdot\nabla\mathbf{F}^T\cdot\hat{\mathbf{v}})+(\mathbf{G}\cdot\nabla\mathbf{F}^T\cdot\hat{\mathbf{v}})^T\\
&+(\mathbf{G}\cdot\nabla\tilde{\mathbf{q}})+(\mathbf{G}\cdot\nabla\tilde{\mathbf{q}})^T\Big)\Big)\cdot\mathbf{G}.\end{aligned}$$

By inserting $\mathbf{F}$, $\mathbf{G}$ and $\tilde{\mathbf{q}}$ of Comp 6 the stress tensor is expressed in the special choice of scaled curvilinear coordinates. The subsequent calculation procedure that is based on pure tensor calculus and the use of Eq (4) is technical and very lengthy. It finally results in the decomposition of $\hat{\mathbf{S}}$ into the mixed basis $\boldsymbol{\eta}_\mathbf{i}\otimes\mathbf{e_j}, i,j=1,2,3$ with $\boldsymbol{\tau}=\boldsymbol{\eta}_\mathbf{3}$ which will turn out to be appropriate for the asymptotical derivation of the one-dimensional fiber model. For further details of the proof we refer to [9].

3.3 Fiber Family in Scaled Curvilinear Coordinates

The scaled curvilinear coordinate transformation is determined by the curve $\boldsymbol{\gamma}$ and the scaling factor ϵ. For the application of the provided theory on the fiber problem we specify these quantities by the center-line of the fiber and the slenderness parameter in Eq (1). This choice has some crucial consequences for the logical structure of our problem. As the dynamics of the center-line depends on the solution of the free BVP, the coordinate transformation becomes part of the problem. To state this point more precisely, we impose the following assumption concerning the fiber domain and its cross-sections.

Assumption 8 (Fiber Geometry)
Let $\Omega(t)$ be the flow domain of the fiber spinning process and ϵ the slenderness parameter of Eq (1). Moreover, let $\boldsymbol{\gamma}(\cdot,t)\colon [0,L(t)) \mapsto \Omega(t)$ for $t \in \mathbb{R}^+$ be a time-dependent arc-length parameterized curve. Then, we assume

- *A scaled curvilinear coordinate transformation $\check{\mathbf{r}}(\cdot,t)\colon \hat{\Omega}(t) \mapsto \Omega(t)$ for $t \in \mathbb{R}^+$ exists with respect to ϵ and $\boldsymbol{\gamma}$.*
- *$\hat{\Omega}(t)$ is given by the fiber length $L(t)$ and the smooth, 2π-periodic radius function $R(\cdot,t) : [0,2\pi) \times [0,L(t)) \mapsto \mathbb{R}^+$ in such a way that*

$$\hat{\Omega}(t) = \{\, \mathbf{x} = (x_1, x_2, s) \in \mathbb{R}^3 \,|\, (x_1,x_2) \in \mathcal{A}(s,t), s \in [0,L(t))\}$$

with cross-sections

$$\mathcal{A}(s,t) = \{(x_1,x_2) \in \mathbb{R}^2 \,|\, x_1 = \varrho\cos(\psi), x_2 = \varrho\sin(\psi), \varrho \in [0,R(\psi,s,t)],\ \psi \in [0,2\pi)\}.$$

- *The curve $\boldsymbol{\gamma}$ satisfies the center-line condition, i.e.*

$$\int_{\mathcal{A}(s,t)} x_1 \,\mathrm{d}x_1\mathrm{d}x_2 = \int_{\mathcal{A}(s,t)} x_2 \,\mathrm{d}x_1\mathrm{d}x_2 = 0.$$

Assumption 8 completely describes the whole fiber domain in the scaled curvilinear coordinates by the three quantities: fiber length L, center-line $\boldsymbol{\gamma}$ and radius function R.

In particular, the lateral surface of the fiber $\hat{\Gamma}_{lat}(t)$ can be parameterized in terms of these quantities by the bijective function $\boldsymbol{\xi}(\cdot,t)\colon [0,2\pi) \times [0,L(t)) \mapsto \hat{\Gamma}_{lat}(t) \subset \mathbb{R}^3$

$$\boldsymbol{\xi}(\psi,s,t) = (R(\psi,s,t)\cos(\psi),\ R(\psi,s,t)\sin(\psi),\ s). \tag{5}$$

Then, the outer normal vector $\hat{\mathbf{n}}$ and the surface speed $\hat{w}$ are expressed by

$$\hat{\mathbf{n}}(\boldsymbol{\xi},t) = \frac{\partial_\psi\boldsymbol{\xi} \times \partial_s\boldsymbol{\xi}}{\parallel \partial_\psi\boldsymbol{\xi} \times \partial_s\boldsymbol{\xi} \parallel}, \qquad \hat{w}(\boldsymbol{\xi},t) = \partial_t\boldsymbol{\xi} \cdot \hat{\mathbf{n}}(\boldsymbol{\xi},t)$$

which leads to the following formulation of the kinematic and dynamic boundary conditions

$$(\hat{\mathbf{v}}(\boldsymbol{\xi},t) - \partial_t\boldsymbol{\xi}) \cdot (\partial_\psi\boldsymbol{\xi} \times \partial_s\boldsymbol{\xi}) = 0, \qquad \hat{\mathbf{S}}(\boldsymbol{\xi},t) \cdot (\partial_\psi\boldsymbol{\xi} \times \partial_s\boldsymbol{\xi})) = \mathbf{0}.$$

As for the bottom boundary $\hat{\Gamma}_{bot}(t) = \mathcal{A}(L(t),t) \times \{L(t)\}$, the outer normal vector is $\mathbf{e_3}$. Hence, the corresponding kinematic and dynamic boundary conditions read

$$\frac{\mathrm{d}L(t)}{\mathrm{d}t} = (\hat{\mathbf{v}} \cdot \mathbf{e_3})(\mathbf{x},t), \qquad (\hat{\mathbf{S}} \cdot \mathbf{e_3})(\mathbf{x},t) = \mathbf{0}.$$

The initial condition $\hat{\Omega}(0) = \emptyset$ of the free BVP is equivalent to $L(0) = 0$ that closes the derived ordinary differential equation for the length. The bottom boundary conditions imply a uniform speed of the bottom face which is consistent to the description of planar surfaces in Ass 8. Due to the linearity of the coordinate transformation in (x_1,x_2) this fact leads to a planar bottom face in the spatial coordinates $\Gamma_{bot}(t)$. On first glance this consequence seems to be physically unreasonable, but note that the bottom surface might also reduce to a single point.

For the coming asymptotic analysis it is necessary to study additionally the inflow in more detail. The inflow boundary Γ_{in} is considered to be planar with center point $\boldsymbol{\gamma}_0$ and inner normal $\boldsymbol{\tau_0}$. In correspondence to Ass 8,

$$\boldsymbol{\gamma}(0,t) = \boldsymbol{\gamma}_0, \qquad \partial_s\boldsymbol{\gamma}(0,t) = \boldsymbol{\tau_0}.$$

Moreover, the relations for inflow velocity profile and slenderness parameter Eqs (1),(2) can be reformulated as

$$|\, \hat{\Gamma}_{in} \,| = |\, \mathcal{A}(0,t) \,| = 1 \tag{6}$$

$$\int_{\hat{\Gamma}_{in}} \tilde{\mathbf{v}}_{in} \cdot \boldsymbol{\tau_0} \,\mathrm{d}\mathcal{A} = \int_{\mathcal{A}(0,t)} \tilde{\mathbf{v}}_{in} \cdot \boldsymbol{\tau_0} \,\mathrm{d}x_1\mathrm{d}x_2 = 1. \tag{7}$$

By the way, the inner normal vector of $\hat{\Gamma}_{in} = \mathcal{A}(0,t) \times \{0\}$ is $\mathbf{e_3}$ and not $\boldsymbol{\tau_0}$.

To analyze the free BVP asymptotically it is embedded for a fixed slenderness parameter $\epsilon = \epsilon_0$ in a family of self-similar problems corresponding to parameters $\epsilon \leq \epsilon_0$. For this family a fixed inflow domain in scaled curvilinear coordinates $(\hat{\Gamma}_{in})_\epsilon = \hat{\Gamma}_{in}$ as well as a fixed inflow velocity $(\tilde{\mathbf{v}}_{in})_\epsilon = \tilde{\mathbf{v}}_{in}$ are chosen. The choice is enabled by the ϵ-independence of Eqs (6),(7). Note that the ϵ-dependence is originally carried into the spatial problem by the boundary description, cf. Eqs (1),(2). Due to the coordinate transformation the boundary conditions in the scaled curvilinear coordinates become independent of ϵ, instead the slenderness parameter occurs explicitely in the balance laws. Summarizing the full set of equations for the fiber family, the variables depending on the slenderness parameter are marked with subscript ϵ.

Balance laws, $\mathbf{x} \in \hat{\Omega}_\epsilon(t)$

$$\partial_t J_\epsilon(\mathbf{x},t) + \nabla_{\mathbf{x}} \cdot (J_\epsilon \hat{\mathbf{v}}_\epsilon)(\mathbf{x},t) = 0$$
$$\partial_t (J_\epsilon \tilde{\mathbf{v}}_\epsilon)(\mathbf{x},t) + \nabla_{\mathbf{x}} \cdot (\hat{\mathbf{v}}_\epsilon \otimes J_\epsilon \tilde{\mathbf{v}}_\epsilon)(\mathbf{x},t) = \nabla_{\mathbf{x}} \cdot \hat{\mathbf{S}}_\epsilon^T(\mathbf{x},t) + (J_\epsilon \tilde{\mathbf{f}}_\epsilon)(\mathbf{x},t)$$

Coupling condition

$$\hat{\mathbf{v}}_\epsilon = (\tilde{\mathbf{v}}_\epsilon - \tilde{\mathbf{q}}_\epsilon) \cdot \mathbf{G}_\epsilon$$

Constitutive law

$$\begin{aligned}
\hat{\mathbf{S}}_\epsilon = -\tilde{p}_\epsilon & \left(\epsilon(1-\epsilon h_\epsilon) \left(\boldsymbol{\eta}_{\alpha,\epsilon} \otimes \mathbf{e}_\alpha\right) + \epsilon^2 \left(\boldsymbol{\tau}_\epsilon \otimes \mathbf{e_3}\right) \right) \\
& + \frac{1}{\mathrm{Re}} \Big(\epsilon(1-\epsilon h_\epsilon) \left(\partial_\alpha(\hat{\mathbf{v}}_\epsilon \cdot \mathbf{e}_\beta) + \partial_\beta(\hat{\mathbf{v}}_\epsilon \cdot \mathbf{e}_\alpha)\right) \ (\boldsymbol{\eta}_{\alpha,\epsilon} \otimes \mathbf{e}_\beta) \\
& \quad + (\epsilon(1-\epsilon h_\epsilon)\partial_\alpha(\hat{\mathbf{v}}_\epsilon \cdot \mathbf{e_3}) + \frac{\epsilon^3}{(1-\epsilon h_\epsilon)} \partial_s(\hat{\mathbf{v}}_\epsilon \cdot \mathbf{e}_\alpha)) \ (\boldsymbol{\eta}_{\alpha,\epsilon} \otimes \mathbf{e_3}) \\
& \quad + \left(\epsilon^2 \partial_s(\hat{\mathbf{v}}_\epsilon \cdot \mathbf{e}_\alpha) + (1-\epsilon h_\epsilon)^2 \partial_\alpha(\hat{\mathbf{v}}_\epsilon \cdot \mathbf{e_3})\right) \ (\boldsymbol{\tau}_\epsilon \otimes \mathbf{e}_\alpha) \\
& \quad + (2\,\epsilon^2 \partial_s(\hat{\mathbf{v}}_\epsilon \cdot \mathbf{e_3}) - \frac{2\epsilon^3}{(1-\epsilon h_\epsilon)} \left(\partial_t h_\epsilon + (\hat{\mathbf{v}}_\epsilon \cdot \mathbf{e}_\alpha)\partial_\alpha h_\epsilon + (\hat{\mathbf{v}}_\epsilon \cdot \mathbf{e_3})\partial_s h_\epsilon\right)) \ (\boldsymbol{\tau}_\epsilon \otimes \mathbf{e_3}) \Big)
\end{aligned}$$

Lateral surface conditions, $\boldsymbol{\xi}_\epsilon \in (\hat{\Gamma}_{lat})_\epsilon(t)$

$$(\hat{\mathbf{v}}_\epsilon(\boldsymbol{\xi}_\epsilon,t) - \partial_t \boldsymbol{\xi}_\epsilon) \cdot (\partial_\psi \boldsymbol{\xi}_\epsilon \times \partial_s \boldsymbol{\xi}_\epsilon) = 0, \qquad \hat{\mathbf{S}}_\epsilon(\boldsymbol{\xi}_\epsilon,t) \cdot (\partial_\psi \boldsymbol{\xi}_\epsilon \times \partial_s \boldsymbol{\xi}_\epsilon)) = \mathbf{0}$$

Bottom surface conditions, $\mathbf{x} \in (\hat{\Gamma}_{bot})_\epsilon(t)$

$$\frac{\mathrm{d}L_\epsilon(t)}{\mathrm{d}t} = (\hat{\mathbf{v}}_\epsilon \cdot \mathbf{e_3})(\mathbf{x},t), \ L_\epsilon(0) = 0, \qquad (\hat{\mathbf{S}}_\epsilon \cdot \mathbf{e_3})(\mathbf{x},t) = \mathbf{0}$$

Inflow boundary condition, $\mathbf{x} \in (\hat{\Gamma}_{in})_\epsilon$

$$\tilde{\mathbf{v}}_\epsilon(\mathbf{x},t) = \tilde{\mathbf{v}}_{in}(\mathbf{x})$$

Geometry conditions

$$\boldsymbol{\gamma}_\epsilon(0,t) = \boldsymbol{\gamma}_0, \qquad \partial_s \boldsymbol{\gamma}_\epsilon(0,t) = \boldsymbol{\tau_0}$$
$$\int\limits_{\mathcal{A}_\epsilon(s,t)} x_1 \ \mathrm{d}x_1 \, \mathrm{d}x_2 = \int\limits_{\mathcal{A}_\epsilon(s,t)} x_2 \ \mathrm{d}x_1 \, \mathrm{d}x_2 = 0$$
$$\| \ \partial_s \boldsymbol{\gamma}_\epsilon \ \| = 1$$

The unknowns are the field variables $\tilde{\mathbf{v}}_\epsilon$, $\hat{\mathbf{v}}_\epsilon$, p_ϵ and the geometry variables L_ϵ, $\boldsymbol{\gamma}_\epsilon$, R_ϵ. All other occurring quantities are defined by the geometry.

4 Asymptotic Analysis

The derivation of the one-dimensional asymptotic fiber model from the three-dimensional free BVP is based on the cross-sectional averaging of the balance laws. Thereby, the asymptotic expansions in zeroth and first order yield the necessary cross-sectional profile properties of the unknowns. The stated asymptotic analysis uses the techniques of [6].

4.1 Cross-sectional Averaging

For the required integration over the cross-sections and their boundary curves, special rules are provided in this section. To facilitate the readability we introduce the following convention

$$\langle f\rangle_{\mathcal{A}(s,t)} = \int\limits_{\mathcal{A}(s,t)} f(x_1,x_2,s,t)\ \mathrm{d}x_1\mathrm{d}x_2$$
$$\langle f\rangle_{\partial\mathcal{A}(s,t)} = \int\limits_{\partial\mathcal{A}(s,t)} \frac{f}{\sqrt{\hat{n}_1^2+\hat{n}_2^2}}\ \mathrm{d}l,$$

where f denotes a differentiable and integrable scalar-, vector- or tensor-valued function on $\hat{\Omega}(t)$, $\mathcal{A}$ a cross-section and $\hat{\mathbf{n}}$ the unit outer normal vector on the free lateral surface $\hat{\Gamma}_{lat}(t)$.

Theorem 9
Let f be a differentiable and integrable scalar-, vector- or tensor-valued function on $\hat{\Omega}(t)$, then the following computation rules are valid

$$\partial_s\langle f\rangle_{\mathcal{A}(s,t)} = \langle\partial_s f\rangle_{\mathcal{A}(s,t)} - \langle f\hat{n}_3\rangle_{\partial\mathcal{A}(s,t)}$$
$$\partial_t\langle f\rangle_{\mathcal{A}(s,t)} = \langle\partial_t f\rangle_{\mathcal{A}(s,t)} + \langle f\hat{w}\rangle_{\partial\mathcal{A}(s,t)}.$$

Proof: A more general version of Th 9 can be concluded from the Reynolds-Transport Theorem according to [6]. However, for our restricted assumptions it is pure calculus using the parameterization of the lateral surface Eq (5).

Corollary 10
Let $\mathbf{m}$ and $\mathbf{M}$ be an arbitrary vector and tensor field with the same properties as f of Th 9. Then

$$\langle\nabla\cdot\mathbf{m}\rangle_{\mathcal{A}(s,t)} = \partial_s\langle\mathbf{m}\cdot\mathbf{e_3}\rangle_{\mathcal{A}(s,t)} + \langle\mathbf{m}\cdot\hat{\mathbf{n}}\rangle_{\partial\mathcal{A}(s,t)}$$
$$\langle\nabla\cdot\mathbf{M}^T\rangle_{\mathcal{A}(s,t)} = \partial_s\langle\mathbf{M}\cdot\mathbf{e_3}\rangle_{\mathcal{A}(s,t)} + \langle\mathbf{M}\cdot\hat{\mathbf{n}}\rangle_{\partial\mathcal{A}(s,t)}.$$

Proof: The corollary results directly from Th 9 using the Gauss Theorem.

Applying the integration rules of Th 9 and Cor 10 on the three-dimensional balance laws of our family problem and incorporating the lateral surface conditions yield one-dimensional balance laws that will play the crucial role for the closing of the asymptotic expansions in the following subsection.

Theorem 11 (Cross-sectional Averaged Balance Laws)
Let a solution of the fiber family BVP exist. Then the following cross-sectional integral relations hold

$$\partial_t\langle J_\epsilon\rangle_{\mathcal{A}_\epsilon(s,t)} + \partial_s\langle J_\epsilon(\hat{\mathbf{v}}_\epsilon\cdot\mathbf{e_3})\rangle_{\mathcal{A}_\epsilon(s,t)} = 0$$
$$\partial_t\langle J_\epsilon\tilde{\mathbf{v}}_\epsilon\rangle_{\mathcal{A}_\epsilon(s,t)} + \partial_s\langle J_\epsilon(\hat{\mathbf{v}}_\epsilon\cdot\mathbf{e_3})\,\tilde{\mathbf{v}}_\epsilon\rangle_{\mathcal{A}_\epsilon(s,t)} = \partial_s\langle\hat{\mathbf{S}}_\epsilon\cdot\mathbf{e_3}\rangle_{\mathcal{A}_\epsilon(s,t)} + \langle J_\epsilon\tilde{\mathbf{f}}_\epsilon\rangle_{\mathcal{A}_\epsilon(s,t)}.$$

4.2 Asymptotic Expansions

The special challenge for the asymptotic expansion of the free BVP equations is the fact that the fiber domain itself depends on ϵ. We tackle this difficulty by extending all field quantities on the domain $\cup_{\epsilon<\epsilon_0}\hat{\Omega}_\epsilon(t)$ and presupposing that their restrictions on $\hat{\Omega}_\epsilon(t)$ are solutions of the respective ϵ-problem.

For the underlying geometry variables, regular power series expansions in ϵ are set up

$$L_\epsilon(t) = L^{(0)}(t) + \epsilon\, L^{(1)}(t) + \mathcal{O}(\epsilon^2)$$
$$\boldsymbol{\gamma}_\epsilon(s,t) = \boldsymbol{\gamma}^{(0)}(s,t) + \epsilon\,\boldsymbol{\gamma}^{(1)}(s,t) + \mathcal{O}(\epsilon^2)$$
$$R_\epsilon(\psi,s,t) = R^{(0)}(\psi,s,t) + \epsilon\, R^{(1)}(\psi,s,t) + \mathcal{O}(\epsilon^2)$$

with $s \in [0, \max_{\epsilon<\epsilon_0} L_\epsilon(t))$ and $\psi \in [0, 2\pi)$. The field variables $\tilde{\mathbf{v}}_\epsilon$ and $\tilde{p}_\epsilon$ are analogously expanded

$$\tilde{\mathbf{v}}_\epsilon(\mathbf{x}, t) = \tilde{\mathbf{v}}^{(0)}(\mathbf{x}, t) + \epsilon\, \tilde{\mathbf{v}}^{(1)}(\mathbf{x}, t) + \mathcal{O}(\epsilon^2)$$
$$\tilde{p}_\epsilon(\mathbf{x}, t) = \tilde{p}^{(0)}(\mathbf{x}, t) + \epsilon\, \tilde{p}^{(1)}(\mathbf{x}, t) + \mathcal{O}(\epsilon^2)$$

for $\mathbf{x} \in \cup_{\epsilon<\epsilon_0} \hat{\Omega}_\epsilon(t)$. Then, the coupling condition determines the expansion of $\hat{\mathbf{v}}$ whose leading order term is $\mathcal{O}(\epsilon^{-1})$ due to the decomposition of $\mathbf{G}_\epsilon = \mathbf{g}_{\mathbf{i},\epsilon} \otimes \mathbf{e_i}$ in Comp 6

$$\hat{\mathbf{v}}_\epsilon(\mathbf{x}, t) = \epsilon^{-1}\, \hat{\mathbf{v}}^{(-1)}(\mathbf{x}, t) + \hat{\mathbf{v}}^{(0)}(\mathbf{x}, t) + \epsilon\, \hat{\mathbf{v}}^{(1)}(\mathbf{x}, t) + \mathcal{O}(\epsilon^2),$$

in particular note

$$\hat{v}_3^{(-1)} = (\hat{\mathbf{v}}^{(-1)} \cdot \mathbf{e_3}) = 0$$

since $\mathbf{g}_{\mathbf{3},\epsilon} \sim \mathcal{O}(1)$. The other two components $\hat{v}_1^{(-1)}$ and $\hat{v}_2^{(-1)}$ will also vanish in the asymptotic analysis. The leading order term of the body force densities is assumed to be $\tilde{\mathbf{f}}^{(0)}$.

It makes no sense to study the asymptotics of the sets $\hat{\Omega}_\epsilon(t)$, $(\hat{\Gamma}_{lat})_\epsilon(t)$, $(\hat{\Gamma}_{bot})_\epsilon(t)$ and $\mathcal{A}_\epsilon(s,t)$ in analogon to the functions. However, the limit case $\epsilon \to 0$ exists and this reference geometry is denoted by $\hat{\Omega}_0(t)$, $(\hat{\Gamma}_{lat})_0(t)$, $(\hat{\Gamma}_{bot})_0(t)$ and $\mathcal{A}_0(s,t)$. The corresponding normal vectors and the surface speed in parametric version are given by

$$\hat{\mathbf{n}}_0(\boldsymbol{\xi}^{(0)}, t) = \frac{\partial_\psi \boldsymbol{\xi}^{(0)} \times \partial_s \boldsymbol{\xi}^{(0)}}{\| \partial_\psi \boldsymbol{\xi}^{(0)} \times \partial_s \boldsymbol{\xi}^{(0)} \|}, \qquad \hat{w}_0(\boldsymbol{\xi}^{(0)}, t) = \boldsymbol{\xi}^{(0)} \cdot \hat{\mathbf{n}}_0(\boldsymbol{\xi}^{(0)}, t).$$

Using Taylor expansion around the reference geometry, the lateral surface conditions read

$$\begin{aligned} 0 =& \hat{\mathbf{v}}^{(-1)}(\boldsymbol{\xi}^{(0)}, t) \cdot (\partial_\psi \boldsymbol{\xi}^{(0)} \times \partial_s \boldsymbol{\xi}^{(0)}) \\ &+ \epsilon \Big((\hat{\mathbf{v}}^{(0)}(\boldsymbol{\xi}^{(0)}, t) + \boldsymbol{\xi}^{(1)} \cdot \nabla \hat{\mathbf{v}}^{(-1)}(\boldsymbol{\xi}^{(0)}, t) - \partial_t \boldsymbol{\xi}^{(0)}) \cdot (\partial_\psi \boldsymbol{\xi}^{(0)} \times \partial_s \boldsymbol{\xi}^{(0)}) \\ &\quad + \hat{\mathbf{v}}^{(-1)}(\boldsymbol{\xi}^{(0)}, t) \cdot (\partial_\psi \boldsymbol{\xi}^{(0)} \times \partial_s \boldsymbol{\xi}^{(1)} + \partial_\psi \boldsymbol{\xi}^{(1)} \times \partial_s \boldsymbol{\xi}^{(0)}) \Big) + \mathcal{O}(\epsilon^2) \end{aligned} \tag{8}$$

and

$$\begin{aligned} \mathbf{0} =& \hat{\mathbf{S}}^{(0)}(\boldsymbol{\xi}^{(0)}, t) \cdot (\partial_\psi \boldsymbol{\xi}^{(0)} \times \partial_s \boldsymbol{\xi}^{(0)}) \\ &+ \epsilon \Big((\hat{\mathbf{S}}^{(1)}(\boldsymbol{\xi}^{(0)}, t) + \boldsymbol{\xi}^{(1)} \cdot \nabla \hat{\mathbf{S}}^{(0)}(\boldsymbol{\xi}^{(0)}, t)) \cdot (\partial_\psi \boldsymbol{\xi}^{(0)} \times \partial_s \boldsymbol{\xi}^{(0)}) \\ &\quad + \hat{\mathbf{S}}^{(0)}(\boldsymbol{\xi}^{(0)}, t) \cdot (\partial_\psi \boldsymbol{\xi}^{(0)} \times \partial_s \boldsymbol{\xi}^{(1)} + \partial_\psi \boldsymbol{\xi}^{(1)} \times \partial_s \boldsymbol{\xi}^{(0)}) \Big) + \mathcal{O}(\epsilon^2). \end{aligned} \tag{9}$$

In the following these equations lead to boundary conditions in zeroth and first order for the reference geometry. Therefore, the unknowns defined on $\cup_{\epsilon<\epsilon_0} \hat{\Omega}_\epsilon(t)$ are assumed to satisfy the balance laws on $\hat{\Omega}_0(t)$.

Focusing on the family balance laws with lateral surface conditions (lateral problem), zeroth and first order equations in ϵ with closure conditions are now derived that result in the desired one-dimensional asymptotic fiber model on the reference geometry. Since the form of the zeroth and first order equations is similar, a general solution theorem is pre-stated.

Theorem 12
Let $\mathcal{D} \subset \mathbb{R}^2$ be a bounded domain with outer normal vector $\mathbf{n}$ on $\partial\mathcal{D}$. Let $g : \mathcal{D} \to \mathbb{R}$ be given. Let $f : \mathcal{D} \to \mathbb{R}$, $\boldsymbol{\Phi} : \mathcal{D} \to \mathbb{R}^2$ and $\varphi : \mathcal{D} \to \mathbb{R}$ be sufficiently smooth.

1. *The solution of the boundary value problem*

$$\begin{aligned} \nabla \cdot \boldsymbol{\Phi} = g, \qquad & \nabla(\nabla \cdot \boldsymbol{\Phi}) + \triangle \boldsymbol{\Phi} = \nabla f && \text{in } \mathcal{D} \\ & (\nabla \boldsymbol{\Phi} + \nabla \boldsymbol{\Phi}^T) \cdot \mathbf{n} = f \mathbf{n} && \text{on } \partial\mathcal{D} \end{aligned}$$

has the form

$$\Phi_1(x_1,x_2)=\frac{g}{2}x_1-ax_2+b_1,\qquad \Phi_2(x_1,x_2)=\frac{g}{2}x_2+ax_1+b_2,\qquad f=g,$$

with constant parameters a, b_1 and b_2.

2. *The solution of the boundary value problem*

$$\triangle\varphi=0\quad \text{in } \mathcal{D},\qquad \nabla\varphi\cdot\mathbf{n}=0\quad \text{on } \partial\mathcal{D}$$

is constant, i.e. $\varphi(x_1,x_2)=c$.

Proof: For the two-dimensional stress-free Stokes equations the solution form is derived in [6], and for the Laplace equation with Neumann condition it is trivial.

Zeroth Order

Using the zeroth order stress tensor

$$\hat{\mathbf{S}}^{(0)}=\frac{1}{\mathrm{Re}}\Big((\partial_\alpha\hat{v}_\beta^{(-1)}+\partial_\beta\hat{v}_\alpha^{(-1)})(\boldsymbol{\eta}_\alpha^{(0)}\otimes\mathbf{e}_\beta)+(\partial_\alpha\hat{v}_3^{(0)})(\boldsymbol{\tau}^{(0)}\otimes\mathbf{e}_\alpha)\Big)$$

and Eqs (8),(9), the balance laws with lateral surface conditions on the reference geometry read

$$\begin{aligned}&\partial_\alpha\hat{\mathbf{v}}_\alpha^{(-1)}=0,\qquad \Big(\partial_{\alpha\beta}\hat{v}_\beta^{(-1)}+\partial_{\beta\beta}\hat{v}_\alpha^{(-1)}\Big)\boldsymbol{\eta}_\alpha^{(0)}+(\partial_{\alpha\alpha}\hat{v}_3^{(0)})\boldsymbol{\tau}^{(0)}=\mathbf{0}\qquad &&\text{in } \hat{\Omega}_0(t)\\ &\qquad\qquad (\partial_\alpha\hat{v}_\beta^{(-1)}+\partial_\beta\hat{v}_\alpha^{(-1)})\hat{n}_{0,\beta}\,\boldsymbol{\eta}_\alpha^{(0)}+\partial_\alpha\hat{v}_3^{(0)}\hat{n}_{0,\alpha}\,\boldsymbol{\tau}^{(0)}=\mathbf{0}\qquad &&\text{on } (\hat{\Gamma}_{lat})_0(t)\end{aligned}$$

Lemma 13 (Cross-sectional Profile Properties in Zeroth Order)
Let the center-line condition be valid and the kinematic boundary condition fulfill $\hat{v}_\alpha^{(-1)}\hat{n}_{0,\alpha}=0$. Then, the solution of the stated zeroth order lateral problem satisfies

$$\hat{v}_1^{(-1)}=\hat{v}_2^{(-1)}\equiv 0,\qquad \hat{v}_3^{(0)}=\hat{v}_3^{(0)}(s,t)$$

Proof: Applying Th 12.1 for $\hat{v}_1^{(-1)}$ and $\hat{v}_2^{(-1)}$ yields

$$\hat{v}_1^{(-1)}=-a(s,t)x_2+b_1(s,t),\qquad \hat{v}_2^{(-1)}=a(s,t)x_1+b_2(s,t).$$

Note that $f=g=0$ are consistently given. The constants $b_1(s,t)$ and $b_2(s,t)$ are determined as $b_1=b_2=0$ by means of the center-line and kinematic boundary condition. Moreover, $a(s,t)$ might vanish or the cross-sections have a circular profile according to the kinematic boundary condition. Since any slight perturbations at the nozzle destroy the circular cross-sectional profile, $a=0$ is the only relevant solution. The result for $\hat{v}_3^{(0)}$ follows directly from Th 12.2.

As consequence of the lemma the zeroth order velocity and stress satisfy

$$\tilde{\mathbf{v}}^{(0)}=\hat{v}_3^{(0)}\boldsymbol{\tau}^{(0)}+\partial_t\boldsymbol{\gamma}^{(0)},\qquad \hat{\mathbf{S}}^{(0)}=\mathbf{0}.$$

The velocity relation being derived from the coupling condition implies $\tilde{\mathbf{v}}^{(0)}=\tilde{\mathbf{v}}^{(0)}(s,t)$, since $\hat{v}_3^{(0)}$ is constant in the cross-sections.

First Order

With the results of zeroth order and the concluded first order stress tensor

$$\hat{\mathbf{S}}^{(1)}=-\tilde{p}^{(0)}(\boldsymbol{\eta}_\alpha^{(0)}\otimes\mathbf{e}_\alpha)+\frac{1}{\mathrm{Re}}\Big((\partial_\alpha\hat{v}_\beta^{(0)}+\partial_\beta\hat{v}_\alpha^{(0)})(\boldsymbol{\eta}_\alpha^{(0)}\otimes\mathbf{e}_\beta)+\partial_\alpha\hat{v}_3^{(1)}(\boldsymbol{\tau}^{(0)}\otimes\mathbf{e}_\alpha)\Big),$$

the first order lateral problem reads

$$\partial_\alpha \hat{v}_\alpha^{(0)} + \partial_s \hat{v}_3^{(0)} = 0, \qquad \left(\partial_{\alpha\beta}\hat{v}_\beta^{(0)} + \partial_{\beta\beta}\hat{v}_\alpha^{(0)} - \mathrm{Re}\ \partial_\alpha \tilde{p}^{(0)}\right)\boldsymbol{\eta}_\alpha^{(0)} + \partial_{\alpha\alpha}\hat{v}_3^{(1)}\boldsymbol{\tau}^{(0)} = \mathbf{0} \quad \text{in } \hat{\Omega}_0(t)$$

$$\left((\partial_\alpha \hat{v}_\beta^{(0)} + \partial_\beta \hat{v}_\alpha^{(0)})\hat{n}_{0,\beta} - \mathrm{Re}\ \tilde{p}^{(0)}\hat{n}_{0,\alpha}\right)\boldsymbol{\eta}_\alpha^{(0)} + \partial_\alpha \hat{v}_3^{(1)}\hat{n}_{0,\alpha}\,\boldsymbol{\tau}^{(0)} = \mathbf{0} \quad \text{on } (\hat{\Gamma}_{lat})_0(t)$$

The validity of the boundary conditions on the reference geometry is concluded from Eqs (8),(9) with $\hat{\mathbf{v}}^{(-1)} = \mathbf{0}$ and $\hat{\mathbf{S}}^{(0)} = \mathbf{0}$.

Lemma 14 (Cross-sectional Profile Properties in First Order)
Let the center-line condition be valid and the kinematic boundary condition fulfill $\hat{v}_\alpha^{(-1)}\hat{n}_{0,\alpha} = \hat{w}_0$. *Then, the solution of the first order lateral problem satisfies*

$$\hat{v}_1^{(0)} = \frac{\mathrm{Re}}{2}\tilde{p}^{(0)}x_1 - a(s,t)x_2 \qquad \tilde{p}^{(0)} = -\frac{1}{\mathrm{Re}}\,\partial_s \hat{v}_3^{(0)}(s,t)$$

$$\hat{v}_2^{(0)} = \frac{\mathrm{Re}}{2}\tilde{p}^{(0)}x_2 + a(s,t)x_1 \qquad \hat{v}_3^{(1)} = \hat{v}_3^{(1)}(s,t).$$

Proof: The strategy of this proof is based on Th 12, analogously to the one for the zeroth order problem.

The determination of $a(s,t)$ is not necessary for our final result. As consequence of the lemma the first order stress satisfies $\hat{\mathbf{S}}^{(1)} = \mathbf{0}$.

Closure

Considering the cross-sectional averaged balance laws of Th 11, only the axial effect of the second order stress tensor is of interest. Using the results of zeroth and first order it particularly reads

$$\hat{\mathbf{S}}^{(2)} \cdot \mathbf{e_3} = \frac{3}{\mathrm{Re}}\,\partial_3 \hat{v}_3^{(0)}\boldsymbol{\tau}^{(0)}.$$

Consequently, the averaged balance laws in their leading order yield the one-dimensional asymptotic fiber model

$$\partial_t \mid \mathcal{A}_0 \mid + \partial_s(\hat{v}_3^{(0)} \mid \mathcal{A}_0 \mid) = 0$$

$$\partial_t(\tilde{\mathbf{v}}^{(0)} \mid \mathcal{A}_0 \mid) + \partial_s(\hat{v}_3^{(0)}\tilde{\mathbf{v}}^{(0)} \mid \mathcal{A}_0 \mid) = \frac{3}{\mathrm{Re}}\,\partial_s(\partial_s \hat{v}_3^{(0)}\boldsymbol{\tau}^{(0)} \mid \mathcal{A}_0 \mid) + \tilde{\mathbf{f}}^{(0)} \mid \mathcal{A}_0 \mid$$

that is closed with the respective coupling, bottom surface, inflow boundary and geometry conditions in leading order

$$\tilde{\mathbf{v}}^{(0)}(s,t) = \hat{v}_3^{(0)}(s,t)\boldsymbol{\tau}^{(0)}(s,t) + \partial_t \boldsymbol{\gamma}^{(0)}(s,t)$$

$$\frac{\mathrm{d}L^{(0)}(t)}{\mathrm{d}t} = \hat{v}_3^{(0)}(L^{(0)}(t),t), \quad L^{(0)}(0) = 0, \qquad \partial_s \hat{v}_3^{(0)}(L(t),t) = 0$$

$$\tilde{\mathbf{v}}^{(0)}(0,t) = \tilde{\mathbf{v}}_{in}(\mathbf{x})$$

$$\boldsymbol{\gamma}^{(0)}(0,t) = \boldsymbol{\gamma}_0, \qquad \partial_s \boldsymbol{\gamma}^{(0)}(0,t) = \boldsymbol{\tau}_0$$

$$\parallel \partial_s \boldsymbol{\gamma}^{(0)} \parallel = 1$$

and additionally

$$\mid \mathcal{A}_0(0,t) \mid = 1.$$

The inflow boundary condition can be reformulated as $\tilde{\mathbf{v}}_{in} = \hat{v}_3^{(0)}(0,t)\boldsymbol{\tau}_0$. Applying Eqs (6),(7) gives then

$$\hat{v}_3^{(0)}(0,t) = 1.$$

5 Fiber Model

Summarizing the asymptotic results, we define $u = \hat{v}_3^{(0)}$, $A =\mid \mathcal{A}_0 \mid$ and drop the superscript at the variables and the body forces of leading order. The resulting one-dimensional model describes the spinning of a slender curved inertial viscous Newtonian fiber. Thereby, it determines the dynamics of the fiber center-line $\boldsymbol{\gamma}$ and the temporal evolution of the fiber length L, the cross-sectional area A, the intrinsic velocity u as well as the velocity $\tilde{\mathbf{v}}$ characterizing the momentum.

Balance laws, $s \in [0, L(t))$

$$\partial_t A + \partial_s(uA) = 0$$

$$\partial_t(A\tilde{\mathbf{v}}) + \partial_s\left(uA\tilde{\mathbf{v}}\right) = \frac{3}{\mathrm{Re}}\,\partial_s\left(A\partial_s u\partial_s\boldsymbol{\gamma}\right) + A\,\tilde{\mathbf{f}}$$

Coupling condition

$$\tilde{\mathbf{v}} = u\,\partial_s\boldsymbol{\gamma} + \partial_t\boldsymbol{\gamma}$$

Boundary condition at the free fiber end

$$\frac{\mathrm{d}L(t)}{\mathrm{d}t} = u(L(t),t),\ L(0) = 0, \qquad \partial_s u(L(t),t) = 0$$

Boundary conditions at the nozzle

$$A(0,t) = 1, \qquad u(0,t) = 1, \qquad \boldsymbol{\gamma}(0,t) = \boldsymbol{\gamma_0}, \qquad \partial_s\boldsymbol{\gamma}(0,t) = \boldsymbol{\tau_0}$$

Geometry constraint

$$\parallel \partial_s\boldsymbol{\gamma} \parallel = 1$$

Our theoretical result coincides with the experimental measurements for a Newtonian fluid by Trouton [10] by retaining the factor 3 in the momentum equation. In dimensional form, this yields the so-called Trouton viscosity 3μ that is already derived in other frameworks [6].

The closure of the underlying free BVP requires the specification of the body forces. In the application of a rotational spinning process the force densities $\mathbf{f}$ stem from gravitation and rotation. In non-dimensionalized form the sum of gravity, coriolis and centrifugal forces reads

$$\mathbf{f}(\mathbf{r},t) = \frac{1}{\mathrm{Fr}^2}\,\mathbf{e_g} - \frac{2}{\mathrm{Rb}}\,(\mathbf{e_\omega} \times \mathbf{v}(\mathbf{r},t)) - \frac{1}{\mathrm{Rb}^2}\,(\mathbf{e_\omega} \times (\mathbf{e_\omega} \times \mathbf{r})),$$

where $g\,\mathbf{e_g} = \mathbf{g}$ denotes the acceleration of gravity and $\omega\,\mathbf{e_\omega} = \boldsymbol{\omega}$ the angular velocity of the rotating device. Thereby, the rotation axis goes through the origin. The dimensionless Froude $\mathrm{Fr} = V/\sqrt{g\ell}$ and Rossby number $\mathrm{Rb} = V/(\omega\ell)$ characterize the relation between inertial and gravitational forces, respectively between inertial and rotational forces. Consequently, the transformed quantity in leading order is given by

$$\tilde{\mathbf{f}} = \frac{1}{\mathrm{Fr}^2}\,\mathbf{e_g} - \frac{2}{\mathrm{Rb}}\,(\mathbf{e_\omega} \times \tilde{\mathbf{v}}) - \frac{1}{\mathrm{Rb}^2}\,(\mathbf{e_\omega} \times (\mathbf{e_\omega} \times \boldsymbol{\gamma})).$$

Aerodynamic forces or surface tension might additionally be incooperated in the model in future. Surface tension will cause a source term in the averaged momentum equations and a change in the boundary conditions at the free fiber end. The momentary neglect of surface tension, $\partial_s u(L(t),t) = 0$, leads together with $\mathrm{d}L(t)/\mathrm{d}t = u(L(t),t)$ to a constant bottom surface since

$$\frac{\mathrm{d}A(L(t),t)}{\mathrm{d}t} = \partial_s(uA)(L(t),t) + \partial_t A(L(t),t) = 0.$$

In particular, together with the chosen initial condition it gives $A(L(t),t) = 1$. For high Reynolds numbers and large fibers, this artifical result occurs separately in a boundary layer

and has no effect on the remaining physically reasonable fiber behavior. Further numerical studies to this point are planned.

Summing up, in this paper we have asymptotically derived an one-dimensional fiber model from the given three-dimensional free BVP. The stated balance laws for mass (cross-section) and momentum combine the unrestricted motion of the fiber center-line with the inner viscous transport. Thereby, the physically reasonable and elegant form of the equations results from the introduction of the vector-valued intrinsic velocity in general coordinates that reduces to the scalar-valued quantity u in the final fiber model.

References

[1] S. S. Antman, *Nonlinear problems of elasticity*, Springer Verlag, 1995.

[2] R. L. Bishop, *There is more than one way to frame a curve*, Amer. Math. Month., 82 (1975), pp. 246–251.

[3] L. J. Cummings and P. D. Howell, *On the evolution of non-axissymetric viscous fibres with surface tension inertia and gravity*, Journal of Fluid Mechanics, 389 (1999), pp. 361–389.

[4] S. P. Decent, M. Simmons, E. Parau, D. Wong, A. King, and L. Partridge, *Liquid jets from a rotating orifice*, in Proceedings of the 5th Int. Conf. on Multiphase Flow, ICMF' 04, Yokohama, Japan, 2004.

[5] J. N. Dewynne, P. D. Howell, and P. Wilmott, *Slender viscous fibers with inertia and gravity*, Quartal Journal of Mechanics and Applied Mathematics, 47 (1994), pp. 541–555.

[6] J. N. Dewynne, J. R. Ockendon, and P. Wilmot, *A systematic derivation of the leading-order equations for extensional flows in slender geometries*, Journal of Fluid Mechanics, 244 (1992), pp. 323–338.

[7] V. M. Entov and A. L. Yarin, *The dynamics of thin liquid jets in air*, Journal of Fluid Mechanics, 140 (1984), pp. 91–111.

[8] P. D. Howell, *Extensional thin layer flows*, PhD thesis, St. Catherine's College, Oxford, 1994.

[9] S. Panda, *The dynamics of viscous fibers*, PhD thesis, Technische Universität Kaiserslautern, 2006, submitted.

[10] F. R. S. Trouton, *On the coefficient of viscous traction and its relation to that of viscosity*, Proceedings of the Royal Society London, A 77 (1906), pp. 426–440.

Acknowledgment
This work has been supported by the Kaiserslautern Excellence Cluster *Dependable Adaptive Systems and Mathematical Modeling*.

Published reports of the Fraunhofer ITWM

The PDF-files of the following reports are available under:
www.itwm.fraunhofer.de/de/zentral__berichte/berichte

1. D. Hietel, K. Steiner, J. Struckmeier

A Finite - Volume Particle Method for Compressible Flows

We derive a new class of particle methods for conservation laws, which are based on numerical flux functions to model the interactions between moving particles. The derivation is similar to that of classical Finite-Volume methods; except that the fixed grid structure in the Finite-Volume method is substituted by so-called mass packets of particles. We give some numerical results on a shock wave solution for Burgers equation as well as the well-known one-dimensional shock tube problem.
(19 pages, 1998)

2. M. Feldmann, S. Seibold

Damage Diagnosis of Rotors: Application of Hilbert Transform and Multi-Hypothesis Testing

In this paper, a combined approach to damage diagnosis of rotors is proposed. The intention is to employ signal-based as well as model-based procedures for an improved detection of size and location of the damage. In a first step, Hilbert transform signal processing techniques allow for a computation of the signal envelope and the instantaneous frequency, so that various types of non-linearities due to a damage may be identified and classified based on measured response data. In a second step, a multi-hypothesis bank of Kalman Filters is employed for the detection of the size and location of the damage based on the information of the type of damage provided by the results of the Hilbert transform.
Keywords: Hilbert transform, damage diagnosis, Kalman filtering, non-linear dynamics
(23 pages, 1998)

3. Y. Ben-Haim, S. Seibold

Robust Reliability of Diagnostic Multi-Hypothesis Algorithms: Application to Rotating Machinery

Damage diagnosis based on a bank of Kalman filters, each one conditioned on a specific hypothesized system condition, is a well recognized and powerful diagnostic tool. This multi-hypothesis approach can be applied to a wide range of damage conditions. In this paper, we will focus on the diagnosis of cracks in rotating machinery. The question we address is: how to optimize the multi-hypothesis algorithm with respect to the uncertainty of the spatial form and location of cracks and their resulting dynamic effects. First, we formulate a measure of the reliability of the diagnostic algorithm, and then we discuss modifications of the diagnostic algorithm for the maximization of the reliability. The reliability of a diagnostic algorithm is measured by the amount of uncertainty consistent with no-failure of the diagnosis. Uncertainty is quantitatively represented with convex models.
Keywords: Robust reliability, convex models, Kalman filtering, multi-hypothesis diagnosis, rotating machinery, crack diagnosis
(24 pages, 1998)

4. F.-Th. Lentes, N. Siedow

Three-dimensional Radiative Heat Transfer in Glass Cooling Processes

For the numerical simulation of 3D radiative heat transfer in glasses and glass melts, practically applicable mathematical methods are needed to handle such problems optimal using workstation class computers. Since the exact solution would require super-computer capabilities we concentrate on approximate solutions with a high degree of accuracy. The following approaches are studied: 3D diffusion approximations and 3D ray-tracing methods.
(23 pages, 1998)

5. A. Klar, R. Wegener

A hierarchy of models for multilane vehicular traffic
Part I: Modeling

In the present paper multilane models for vehicular traffic are considered. A microscopic multilane model based on reaction thresholds is developed. Based on this model an Enskog like kinetic model is developed. In particular, care is taken to incorporate the correlations between the vehicles. From the kinetic model a fluid dynamic model is derived. The macroscopic coefficients are deduced from the underlying kinetic model. Numerical simulations are presented for all three levels of description in [10]. Moreover, a comparison of the results is given there.
(23 pages, 1998)

Part II: Numerical and stochastic investigations

In this paper the work presented in [6] is continued. The present paper contains detailed numerical investigations of the models developed there. A numerical method to treat the kinetic equations obtained in [6] are presented and results of the simulations are shown. Moreover, the stochastic correlation model used in [6] is described and investigated in more detail.
(17 pages, 1998)

6. A. Klar, N. Siedow

Boundary Layers and Domain Decomposition for Radiative Heat Transfer and Diffusion Equations: Applications to Glass Manufacturing Processes

In this paper domain decomposition methods for radiative transfer problems including conductive heat transfer are treated. The paper focuses on semi-transparent materials, like glass, and the associated conditions at the interface between the materials. Using asymptotic analysis we derive conditions for the coupling of the radiative transfer equations and a diffusion approximation. Several test cases are treated and a problem appearing in glass manufacturing processes is computed. The results clearly show the advantages of a domain decomposition approach. Accuracy equivalent to the solution of the global radiative transfer solution is achieved, whereas computation time is strongly reduced.
(24 pages, 1998)

7. I. Choquet

Heterogeneous catalysis modelling and numerical simulation in rarified gas flows
Part I: Coverage locally at equilibrium

A new approach is proposed to model and simulate numerically heterogeneous catalysis in rarefied gas flows. It is developed to satisfy all together the following points:
1) describe the gas phase at the microscopic scale, as required in rarefied flows,
2) describe the wall at the macroscopic scale, to avoid prohibitive computational costs and consider not only crystalline but also amorphous surfaces,
3) reproduce on average macroscopic laws correlated with experimental results and
4) derive analytic models in a systematic and exact way.
The problem is stated in the general framework of a non static flow in the vicinity of a catalytic and non porous surface (without aging). It is shown that the exact and systematic resolution method based on the Laplace transform, introduced previously by the author to model collisions in the gas phase, can be extended to the present problem. The proposed approach is applied to the modelling of the EleyRideal and LangmuirHinshelwood recombinations, assuming that the coverage is locally at equilibrium. The models are developed considering one atomic species and extended to the general case of several atomic species. Numerical calculations show that the models derived in this way reproduce with accuracy behaviors observed experimentally.
(24 pages, 1998)

8. J. Ohser, B. Steinbach, C. Lang

Efficient Texture Analysis of Binary Images

A new method of determining some characteristics of binary images is proposed based on a special linear filtering. This technique enables the estimation of the area fraction, the specific line length, and the specific integral of curvature. Furthermore, the specific length of the total projection is obtained, which gives detailed information about the texture of the image. The influence of lateral and directional resolution depending on the size of the applied filter mask is discussed in detail. The technique includes a method of increasing directional resolution for texture analysis while keeping lateral resolution as high as possible.
(17 pages, 1998)

9. J. Orlik

Homogenization for viscoelasticity of the integral type with aging and shrinkage

A multiphase composite with periodic distributed inclusions with a smooth boundary is considered in this contribution. The composite component materials are supposed to be linear viscoelastic and aging (of the nonconvolution integral type, for which the Laplace transform with respect to time is not effectively applicable) and are subjected to isotropic shrinkage. The free shrinkage deformation can be considered as a fictitious temperature deformation in the behavior law. The procedure presented in this paper proposes a way to determine average (effective homogenized) viscoelastic and shrinkage (temperature) composite properties and the homogenized stressfield from known properties of the components. This is done by the extension of the asymptotic homogenization technique known for pure elastic nonhomogeneous bodies to the nonhomogeneous thermoviscoelasticity of the integral nonconvolution type. Up to now, the homogenization theory has not covered viscoelasticity of the integral type. SanchezPalencia (1980), Francfort & Suquet (1987) (see [2], [9]) have considered homogenization for viscoelasticity of the differential form and only up to the first derivative order. The integralmodeled viscoelasticity is more general then the differential one and includes almost all known differential models. The homogenization procedure is based on the construction of an asymptotic solution with respect to a period of the composite structure. This reduces the original problem to some auxiliary boundary value problems of elasticity and viscoelasticity on the unit periodic cell, of the same type as the original non-homogeneous problem. The existence and uniqueness results for such problems were obtained for kernels satisfying some constrain conditions. This is done by the extension of the Volterra integral operator theory to the Volterra operators with respect to the time, whose 1 kernels are space linear operators for any fixed time variables. Some ideas of such approach were proposed in [11] and [12], where the Volterra operators with kernels depending additionally on parameter were considered. This manuscript delivers results of the same nature for the case of the spaceoperator kernels.
(20 pages, 1998)

10. J. Mohring

Helmholtz Resonators with Large Aperture

The lowest resonant frequency of a cavity resonator is usually approximated by the classical Helmholtz formula. However, if the opening is rather large and the front wall is narrow this formula is no longer valid. Here we present a correction which is of third order in the ratio of the diameters of aperture and cavity. In addition to the high accuracy it allows to estimate the damping due to radiation. The result is found by applying the method of matched asymptotic expansions. The correction contains form factors describing the shapes of opening and cavity. They are computed for a number of standard geometries. Results are compared with numerical computations.
(21 pages, 1998)

11. H. W. Hamacher, A. Schöbel

On Center Cycles in Grid Graphs

Finding "good" cycles in graphs is a problem of great interest in graph theory as well as in locational analysis. We show that the center and median problems are NP hard in general graphs. This result holds both for the variable cardinality case (i.e. all cycles of the graph are considered) and the fixed cardinality case (i.e. only cycles with a given cardinality p are feasible). Hence it is of interest to investigate special cases where the problem is solvable in polynomial time. In grid graphs, the variable cardinality case is, for instance, trivially solvable if the shape of the cycle can be chosen freely.
If the shape is fixed to be a rectangle one can analyze rectangles in grid graphs with, in sequence, fixed dimension, fixed cardinality, and variable cardinality. In all cases a complete characterization of the optimal cycles and closed form expressions of the optimal objective values are given, yielding polynomial time algorithms for all cases of center rectangle problems.
Finally, it is shown that center cycles can be chosen as rectangles for small cardinalities such that the center cycle problem in grid graphs is in these cases completely solved.
(15 pages, 1998)

12. H. W. Hamacher, K.-H. Küfer

Inverse radiation therapy planning - a multiple objective optimisation approach

For some decades radiation therapy has been proved successful in cancer treatment. It is the major task of clinical radiation treatment planning to realize on the one hand a high level dose of radiation in the cancer tissue in order to obtain maximum tumor control. On the other hand it is obvious that it is absolutely necessary to keep in the tissue outside the tumor, particularly in organs at risk, the unavoidable radiation as low as possible.
No doubt, these two objectives of treatment planning - high level dose in the tumor, low radiation outside the tumor - have a basically contradictory nature. Therefore, it is no surprise that inverse mathematical models with dose distribution bounds tend to be infeasible in most cases. Thus, there is need for approximations compromising between overdosing the organs at risk and underdosing the target volume.
Differing from the currently used time consuming iterative approach, which measures deviation from an ideal (non-achievable) treatment plan using recursively trial-and-error weights for the organs of interest, we go a new way trying to avoid a priori weight choices and consider the treatment planning problem as a multiple objective linear programming problem: with each organ of interest, target tissue as well as organs at risk, we associate an objective function measuring the maximal deviation from the prescribed doses.
We build up a data base of relatively few efficient solutions representing and approximating the variety of Pareto solutions of the multiple objective linear programming problem. This data base can be easily scanned by physicians looking for an adequate treatment plan with the aid of an appropriate online tool.
(14 pages, 1999)

13. C. Lang, J. Ohser, R. Hilfer

On the Analysis of Spatial Binary Images

This paper deals with the characterization of microscopically heterogeneous, but macroscopically homogeneous spatial structures. A new method is presented which is strictly based on integral-geometric formulae such as Crofton's intersection formulae and Hadwiger's recursive definition of the Euler number. The corresponding algorithms have clear advantages over other techniques. As an example of application we consider the analysis of spatial digital images produced by means of Computer Assisted Tomography.
(20 pages, 1999)

14. M. Junk

On the Construction of Discrete Equilibrium Distributions for Kinetic Schemes

A general approach to the construction of discrete equilibrium distributions is presented. Such distribution functions can be used to set up Kinetic Schemes as well as Lattice Boltzmann methods. The general principles are also applied to the construction of Chapman Enskog distributions which are used in Kinetic Schemes for compressible Navier-Stokes equations.
(24 pages, 1999)

15. M. Junk, S. V. Raghurame Rao

A new discrete velocity method for Navier-Stokes equations

The relation between the Lattice Boltzmann Method, which has recently become popular, and the Kinetic Schemes, which are routinely used in Computational Fluid Dynamics, is explored. A new discrete velocity model for the numerical solution of Navier-Stokes equations for incompressible fluid flow is presented by combining both the approaches. The new scheme can be interpreted as a pseudo-compressibility method and, for a particular choice of parameters, this interpretation carries over to the Lattice Boltzmann Method.
(20 pages, 1999)

16. H. Neunzert

Mathematics as a Key to Key Technologies

The main part of this paper will consist of examples, how mathematics really helps to solve industrial problems; these examples are taken from our Institute for Industrial Mathematics, from research in the Technomathematics group at my university, but also from ECMI groups and a company called TecMath, which originated 10 years ago from my university group and has already a very successful history.
(39 pages (4 PDF-Files), 1999)

17. J. Ohser, K. Sandau

Considerations about the Estimation of the Size Distribution in Wicksell's Corpuscle Problem

Wicksell's corpuscle problem deals with the estimation of the size distribution of a population of particles, all having the same shape, using a lower dimensional sampling probe. This problem was originary formulated for particle systems occurring in life sciences but its solution is of actual and increasing interest in materials science. From a mathematical point of view, Wicksell's problem is an inverse problem where the interesting size distribution is the unknown part of a Volterra equation. The problem is often regarded ill-posed, because the structure of the integrand implies unstable numerical solutions. The accuracy of the numerical solutions is considered here using the condition number, which allows to compare different numerical methods with different (equidistant) class sizes and which indicates, as one result, that a finite section thickness of the probe reduces the numerical problems. Furthermore, the relative error of estimation is computed which can be split into two parts. One part consists of the relative discretization error that increases for increasing class size, and the second part is related to the relative statistical error which increases with decreasing class size. For both parts, upper bounds can be given and the sum of them indicates an optimal class width depending on some specific constants.
(18 pages, 1999)

18. E. Carrizosa, H. W. Hamacher, R. Klein, S. Nickel

Solving nonconvex planar location problems by finite dominating sets

It is well-known that some of the classical location problems with polyhedral gauges can be solved in polynomial time by finding a finite dominating set, i. e. a finite set of candidates guaranteed to contain at least one optimal location.
In this paper it is first established that this result holds for a much larger class of problems than currently considered in the literature. The model for which this result can be proven includes, for instance, location problems with attraction and repulsion, and location-allocation problems.
Next, it is shown that the approximation of general gauges by polyhedral ones in the objective function of our general model can be analyzed with regard to the subsequent error in the optimal objective value. For the approximation problem two different approaches are described, the sandwich procedure and the greedy algorithm. Both of these approaches lead - for fixed epsilon - to polynomial approximation algorithms with accuracy epsilon for solving the general model considered in this paper.
Keywords: Continuous Location, Polyhedral Gauges, Finite Dominating Sets, Approximation, Sandwich Algorithm, Greedy Algorithm
(19 pages, 2000)

19. A. Becker

A Review on Image Distortion Measures

Within this paper we review image distortion measures. A distortion measure is a criterion that assigns a "quality number" to an image. We distinguish between mathematical distortion measures and those distortion measures in-cooperating a priori knowledge about the imaging devices (e. g. satellite images), image processing algorithms or the human physiology. We will consider representative examples of different kinds of distortion measures and are going to discuss them.
Keywords: Distortion measure, human visual system
(26 pages, 2000)

20. H. W. Hamacher, M. Labbé, S. Nickel, T. Sonneborn

Polyhedral Properties of the Uncapacitated Multiple Allocation Hub Location Problem

We examine the feasibility polyhedron of the uncapacitated hub location problem (UHL) with multiple allocation, which has applications in the fields of air passenger and cargo transportation, telecommunication and postal delivery services. In particular we determine the dimension and derive some classes of facets of this polyhedron. We develop some general rules about lifting facets from the uncapacitated facility location (UFL) for UHL and projecting facets from UHL to UFL. By applying these rules we get a new class of facets for UHL which dominates the inequalities in the original formulation. Thus we get a new formulation of UHL whose constraints are all facet–defining. We show its superior computational performance by benchmarking it on a well known data set.
Keywords: integer programming, hub location, facility location, valid inequalities, facets, branch and cut
(21 pages, 2000)

21. H. W. Hamacher, A. Schöbel

Design of Zone Tariff Systems in Public Transportation

Given a public transportation system represented by its stops and direct connections between stops, we consider two problems dealing with the prices for the customers: The fare problem in which subsets of stops are already aggregated to zones and "good" tariffs have to be found in the existing zone system. Closed form solutions for the fare problem are presented for three objective functions. In the zone problem the design of the zones is part of the problem. This problem is NP hard and we therefore propose three heuristics which prove to be very successful in the redesign of one of Germany's transportation systems.
(30 pages, 2001)

22. D. Hietel, M. Junk, R. Keck, D. Teleaga

The Finite-Volume-Particle Method for Conservation Laws

In the Finite-Volume-Particle Method (FVPM), the weak formulation of a hyperbolic conservation law is discretized by restricting it to a discrete set of test functions. In contrast to the usual Finite-Volume approach, the test functions are not taken as characteristic functions of the control volumes in a spatial grid, but are chosen from a partition of unity with smooth and overlapping partition functions (the particles), which can even move along pre- scribed velocity fields. The information exchange between particles is based on standard numerical flux functions. Geometrical information, similar to the surface area of the cell faces in the Finite-Volume Method and the corresponding normal directions are given as integral quantities of the partition functions. After a brief derivation of the Finite-Volume-Particle Method, this work focuses on the role of the geometric coefficients in the scheme.
(16 pages, 2001)

23. T. Bender, H. Hennes, J. Kalcsics, M. T. Melo, S. Nickel

Location Software and Interface with GIS and Supply Chain Management

The objective of this paper is to bridge the gap between location theory and practice. To meet this objective focus is given to the development of software capable of addressing the different needs of a wide group of users. There is a very active community on location theory encompassing many research fields such as operations research, computer science, mathematics, engineering, geography, economics and marketing. As a result, people working on facility location problems have a very diverse background and also different needs regarding the software to solve these problems. For those interested in non-commercial applications (e. g. students and researchers), the library of location algorithms (LoLA can be of considerable assistance. LoLA contains a collection of efficient algorithms for solving planar, network and discrete facility location problems. In this paper, a detailed description of the functionality of LoLA is presented. In the fields of geography and marketing, for instance, solving facility location problems requires using large amounts of demographic data. Hence, members of these groups (e. g. urban planners and sales managers) often work with geographical information too s. To address the specific needs of these users, LoLA was inked to a geographical information system (GIS) and the details of the combined functionality are described in the paper. Finally, there is a wide group of practitioners who need to solve large problems and require special purpose software with a good data interface. Many of such users can be found, for example, in the area of supply chain management (SCM). Logistics activities involved in strategic SCM include, among others, facility location planning. In this paper, the development of a commercial location software tool is also described. The too is embedded in the Advanced Planner and Optimizer SCM software developed by SAP AG, Walldorf, Germany. The paper ends with some conclusions and an outlook to future activities.

Keywords: facility location, software development, geographical information systems, supply chain management

(48 pages, 2001)

24. H. W. Hamacher, S. A. Tjandra

Mathematical Modelling of Evacuation Problems: A State of Art

This paper details models and algorithms which can be applied to evacuation problems. While it concentrates on building evacuation many of the results are applicable also to regional evacuation. All models consider the time as main parameter, where the travel time between components of the building is part of the input and the overall evacuation time is the output. The paper distinguishes between macroscopic and microscopic evacuation models both of which are able to capture the evacuees' movement over time.

Macroscopic models are mainly used to produce good lower bounds for the evacuation time and do not consider any individual behavior during the emergency situation. These bounds can be used to analyze existing buildings or help in the design phase of planning a building. Macroscopic approaches which are based on dynamic network flow models (minimum cost dynamic flow, maximum dynamic flow, universal maximum flow, quickest path and quickest flow) are described. A special feature of the presented approach is the fact, that travel times of evacuees are not restricted to be constant, but may be density dependent. Using multicriteria optimization priority regions and blockage due to fire or smoke may be considered. It is shown how the modelling can be done using time parameter either as discrete or continuous parameter.

Microscopic models are able to model the individual evacuee's characteristics and the interaction among evacuees which influence their movement. Due to the corresponding huge amount of data one uses simulation approaches. Some probabilistic laws for individual evacuee's movement are presented. Moreover ideas to model the evacuee's movement using cellular automata (CA) and resulting software are presented.

In this paper we will focus on macroscopic models and only summarize some of the results of the microscopic approach. While most of the results are applicable to general evacuation situations, we concentrate on building evacuation.

(44 pages, 2001)

25. J. Kuhnert, S. Tiwari

Grid free method for solving the Poisson equation

A Grid free method for solving the Poisson equation is presented. This is an iterative method. The method is based on the weighted least squares approximation in which the Poisson equation is enforced to be satisfied in every iterations. The boundary conditions can also be enforced in the iteration process. This is a local approximation procedure. The Dirichlet, Neumann and mixed boundary value problems on a unit square are presented and the analytical solutions are compared with the exact solutions. Both solutions matched perfectly.

Keywords: Poisson equation, Least squares method, Grid free method

(19 pages, 2001)

26. T. Götz, H. Rave, D. Reinel-Bitzer, K. Steiner, H. Tiemeier

Simulation of the fiber spinning process

To simulate the influence of process parameters to the melt spinning process a fiber model is used and coupled with CFD calculations of the quench air flow. In the fiber model energy, momentum and mass balance are solved for the polymer mass flow. To calculate the quench air the Lattice Boltzmann method is used. Simulations and experiments for different process parameters and hole configurations are compared and show a good agreement.

Keywords: Melt spinning, fiber model, Lattice Boltzmann, CFD

(19 pages, 2001)

27. A. Zemitis

On interaction of a liquid film with an obstacle

In this paper mathematical models for liquid films generated by impinging jets are discussed. Attention is stressed to the interaction of the liquid film with some obstacle. S. G. Taylor [Proc. R. Soc. London Ser. A 253, 313 (1959)] found that the liquid film generated by impinging jets is very sensitive to properties of the wire which was used as an obstacle. The aim of this presentation is to propose a modification of the Taylor's model, which allows to simulate the film shape in cases, when the angle between jets is different from 180°. Numerical results obtained by discussed models give two different shapes of the liquid film similar as in Taylors experiments. These two shapes depend on the regime: either droplets are produced close to the obstacle or not. The difference between two regimes becomes larger if the angle between jets decreases. Existence of such two regimes can be very essential for some applications of impinging jets, if the generated liquid film can have a contact with obstacles.

Keywords: impinging jets, liquid film, models, numerical solution, shape

(22 pages, 2001)

28. I. Ginzburg, K. Steiner

Free surface lattice-Boltzmann method to model the filling of expanding cavities by Bingham Fluids

The filling process of viscoplastic metal alloys and plastics in expanding cavities is modelled using the lattice Boltzmann method in two and three dimensions. These models combine the regularized Bingham model for viscoplastic with a free-interface algorithm. The latter is based on a modified immiscible lattice Boltzmann model in which one species is the fluid and the other one is considered as vacuum. The boundary conditions at the curved liquid-vacuum interface are met without any geometrical front reconstruction from a first-order Chapman-Enskog expansion. The numerical results obtained with these models are found in good agreement with available theoretical and numerical analysis.

Keywords: Generalized LBE, free-surface phenomena, interface boundary conditions, filling processes, Bingham viscoplastic model, regularized models

(22 pages, 2001)

29. H. Neunzert

»Denn nichts ist für den Menschen als Menschen etwas wert, was er nicht mit Leidenschaft tun kann«
Vortrag anlässlich der Verleihung des Akademiepreises des Landes Rheinland-Pfalz am 21.11.2001

Was macht einen guten Hochschullehrer aus? Auf diese Frage gibt es sicher viele verschiedene, fachbezogene Antworten, aber auch ein paar allgemeine Gesichtspunkte: es bedarf der »Leidenschaft« für die Forschung (Max Weber), aus der dann auch die Begeisterung für die Lehre erwächst. Forschung und Lehre gehören zusammen, um die Wissenschaft als lebendiges Tun vermitteln zu können. Der Vortrag gibt Beispiele dafür, wie in angewandter Mathematik Forschungsaufgaben aus praktischen Alltagsproblemstellungen erwachsen, die in die Lehre auf verschiedenen Stufen (Gymnasium bis Graduiertenkolleg) einfließen; er leitet damit auch zu einem aktuellen Forschungsgebiet, der Mehrskalenanalyse mit ihren vielfältigen Anwendungen in Bildverarbeitung, Materialentwicklung und Strömungsmechanik über, was aber nur kurz gestreift wird. Mathematik erscheint hier als eine moderne Schlüsseltechnologie, die aber auch enge Beziehungen zu den Geistes- und Sozialwissenschaften hat.

Keywords: Lehre, Forschung, angewandte Mathematik, Mehrskalenanalyse, Strömungsmechanik

(18 pages, 2001)

30. J. Kuhnert, S. Tiwari

Finite pointset method based on the projection method for simulations of the incompressible Navier-Stokes equations

A Lagrangian particle scheme is applied to the projection method for the incompressible Navier-Stokes equations. The approximation of spatial derivatives is obtained by the weighted least squares method. The pressure Poisson equation is solved by a local iterative procedure with the help of the least squares method. Numerical tests are performed for two dimensional cases. The Couette flow, Poiseuelle flow, decaying shear flow and the driven cavity flow are presented. The numerical solutions are obtained for stationary as well as instationary cases and are compared with the analytical solutions for channel flows. Finally, the driven cavity in a unit square is considered and the stationary solution obtained from this scheme is compared with that from the finite element method.

Keywords: Incompressible Navier-Stokes equations, Meshfree method, Projection method, Particle scheme, Least squares approximation

AMS subject classification: 76D05, 76M28

(25 pages, 2001)

31. R. Korn, M. Krekel

Optimal Portfolios with Fixed Consumption or Income Streams

We consider some portfolio optimisation problems where either the investor has a desire for an a priori specified consumption stream or/and follows a deterministic pay in scheme while also trying to maximize expected utility from final wealth. We derive explicit closed form solutions for continuous and discrete monetary streams. The mathematical method used is classical stochastic control theory.

Keywords: Portfolio optimisation, stochastic control, HJB equation, discretisation of control problems.

(23 pages, 2002)

32. M. Krekel

Optimal portfolios with a loan dependent credit spread

If an investor borrows money he generally has to pay higher interest rates than he would have received, if he had put his funds on a savings account. The classical model of continuous time portfolio optimisation ignores this effect. Since there is obviously a connection between the default probability and the total per-

centage of wealth, which the investor is in debt, we study portfolio optimisation with a control dependent interest rate. Assuming a logarithmic and a power utility function, respectively, we prove explicit formulae of the optimal control.
Keywords: Portfolio optimisation, stochastic control, HJB equation, credit spread, log utility, power utility, non-linear wealth dynamics
(25 pages, 2002)

33. J. Ohser, W. Nagel, K. Schladitz

The Euler number of discretized sets - on the choice of adjacency in homogeneous lattices

Two approaches for determining the Euler-Poincaré characteristic of a set observed on lattice points are considered in the context of image analysis { the integral geometric and the polyhedral approach. Information about the set is assumed to be available on lattice points only. In order to retain properties of the Euler number and to provide a good approximation of the true Euler number of the original set in the Euclidean space, the appropriate choice of adjacency in the lattice for the set and its background is crucial. Adjacencies are defined using tessellations of the whole space into polyhedrons. In R 3 , two new 14 adjacencies are introduced additionally to the well known 6 and 26 adjacencies. For the Euler number of a set and its complement, a consistency relation holds. Each of the pairs of adjacencies (14:1; 14:1), (14:2; 14:2), (6; 26), and (26; 6) is shown to be a pair of complementary adjacencies with respect to this relation. That is, the approximations of the Euler numbers are consistent if the set and its background (complement) are equipped with this pair of adjacencies. Furthermore, sufficient conditions for the correctness of the approximations of the Euler number are given. The analysis of selected microstructures and a simulation study illustrate how the estimated Euler number depends on the chosen adjacency. It also shows that there is not a uniquely best pair of adjacencies with respect to the estimation of the Euler number of a set in Euclidean space.
Keywords: image analysis, Euler number, neighborhod relationships, cuboidal lattice
(32 pages, 2002)

34. I. Ginzburg, K. Steiner

Lattice Boltzmann Model for Free-Surface flow and Its Application to Filling Process in Casting

A generalized lattice Boltzmann model to simulate free-surface is constructed in both two and three dimensions. The proposed model satisfies the interfacial boundary conditions accurately. A distinctive feature of the model is that the collision processes is carried out only on the points occupied partially or fully by the fluid. To maintain a sharp interfacial front, the method includes an anti-diffusion algorithm. The unknown distribution functions at the interfacial region are constructed according to the first order Chapman-Enskog analysis. The interfacial boundary conditions are satisfied exactly by the coefficients in the Chapman-Enskog expansion. The distribution functions are naturally expressed in the local interfacial coordinates. The macroscopic quantities at the interface are extracted from the least-square solutions of a locally linearized system obtained from the known distribution functions. The proposed method does not require any geometric front construction and is robust for any interfacial topology. Simulation results of realistic filling process are presented: rectangular cavity in two dimensions and Hammer box, Campbell box, Sheffield box, and Motorblock in three dimensions. To enhance the stability at high Reynolds numbers, various upwind-type schemes are developed. Free-slip and no-slip boundary conditions are also discussed.
Keywords: Lattice Boltzmann models; free-surface phenomena; interface boundary conditions; filling processes; injection molding; volume of fluid method; interface boundary conditions; advection-schemes; upwind-schemes
(54 pages, 2002)

35. M. Günther, A. Klar, T. Materne, R. Wegener

Multivalued fundamental diagrams and stop and go waves for continuum traffic equations

In the present paper a kinetic model for vehicular traffic leading to multivalued fundamental diagrams is developed and investigated in detail. For this model phase transitions can appear depending on the local density and velocity of the flow. A derivation of associated macroscopic traffic equations from the kinetic equation is given. Moreover, numerical experiments show the appearance of stop and go waves for highway traffic with a bottleneck.
Keywords: traffic flow, macroscopic equations, kinetic derivation, multivalued fundamental diagram, stop and go waves, phase transitions
(25 pages, 2002)

36. S. Feldmann, P. Lang, D. Prätzel-Wolters

Parameter influence on the zeros of network determinants

To a network N(q) with determinant D(s;q) depending on a parameter vector q Î Rr via identification of some of its vertices, a network N^ (q) is assigned. The paper deals with procedures to find N^ (q), such that its determinant D^ (s;q) admits a factorization in the determinants of appropriate subnetworks, and with the estimation of the deviation of the zeros of D^ from the zeros of D. To solve the estimation problem state space methods are applied.
Keywords: Networks, Equicofactor matrix polynomials, Realization theory, Matrix perturbation theory
(30 pages, 2002)

37. K. Koch, J. Ohser, K. Schladitz

Spectral theory for random closed sets and estimating the covariance via frequency space

A spectral theory for stationary random closed sets is developed and provided with a sound mathematical basis. Definition and proof of existence of the Bartlett spectrum of a stationary random closed set as well as the proof of a Wiener-Khintchine theorem for the power spectrum are used to two ends: First, well known second order characteristics like the covariance can be estimated faster than usual via frequency space. Second, the Bartlett spectrum and the power spectrum can be used as second order characteristics in frequency space. Examples show, that in some cases information about the random closed set is easier to obtain from these characteristics in frequency space than from their real world counterparts.
Keywords: Random set, Bartlett spectrum, fast Fourier transform, power spectrum
(28 pages, 2002)

38. D. d'Humières, I. Ginzburg

Multi-reflection boundary conditions for lattice Boltzmann models

We present a unified approach of several boundary conditions for lattice Boltzmann models. Its general framework is a generalization of previously introduced schemes such as the bounce-back rule, linear or quadratic interpolations, etc. The objectives are two fold: first to give theoretical tools to study the existing boundary conditions and their corresponding accuracy; secondly to design formally third- order accurate boundary conditions for general flows. Using these boundary conditions, Couette and Poiseuille flows are exact solution of the lattice Boltzmann models for a Reynolds number Re = 0 (Stokes limit).
Numerical comparisons are given for Stokes flows in periodic arrays of spheres and cylinders, linear periodic array of cylinders between moving plates and for Navier-Stokes flows in periodic arrays of cylinders for Re < 200. These results show a significant improvement of the overall accuracy when using the linear interpolations instead of the bounce-back reflection (up to an order of magnitude on the hydrodynamics fields). Further improvement is achieved with the new multi-reflection boundary conditions, reaching a level of accuracy close to the quasi-analytical reference solutions, even for rather modest grid resolutions and few points in the narrowest channels. More important, the pressure and velocity fields in the vicinity of the obstacles are much smoother with multi-reflection than with the other boundary conditions.
Finally the good stability of these schemes is highlighted by some simulations of moving obstacles: a cylinder between flat walls and a sphere in a cylinder.
Keywords: lattice Boltzmann equation, boudary condistions, bounce-back rule, Navier-Stokes equation
(72 pages, 2002)

39. R. Korn

Elementare Finanzmathematik

Im Rahmen dieser Arbeit soll eine elementar gehaltene Einführung in die Aufgabenstellungen und Prinzipien der modernen Finanzmathematik gegeben werden. Insbesondere werden die Grundlagen der Modellierung von Aktienkursen, der Bewertung von Optionen und der Portfolio-Optimierung vorgestellt. Natürlich können die verwendeten Methoden und die entwickelte Theorie nicht in voller Allgemeinheit für den Schulunterricht verwendet werden, doch sollen einzelne Prinzipien so heraus gearbeitet werden, dass sie auch an einfachen Beispielen verstanden werden können.
Keywords: Finanzmathematik, Aktien, Optionen, Portfolio-Optimierung, Börse, Lehrerweiterbildung, Mathematikunterricht
(98 pages, 2002)

40. J. Kallrath, M. C. Müller, S. Nickel

Batch Presorting Problems: Models and Complexity Results

In this paper we consider short term storage systems. We analyze presorting strategies to improve the effiency of these storage systems. The presorting task is called Batch PreSorting Problem (BPSP). The BPSP is a variation of an assigment problem, i. e., it has an assigment problem kernel and some additional constraints. We present different types of these presorting problems, introduce mathematical programming formulations and prove the NP-completeness for one type of the BPSP. Experiments are carried out in order to compare the different model formulations and to investigate the behavior of these models.
Keywords: Complexity theory, Integer programming, Assigment, Logistics
(19 pages, 2002)

41. J. Linn

On the frame-invariant description of the phase space of the Folgar-Tucker equation

The Folgar-Tucker equation is used in flow simulations of fiber suspensions to predict fiber orientation depending on the local flow. In this paper, a complete, frame-invariant description of the phase space of this differential equation is presented for the first time.
Key words: fiber orientation, Folgar-Tucker equation, injection molding
(5 pages, 2003)

42. T. Hanne, S. Nickel

A Multi-Objective Evolutionary Algorithm for Scheduling and Inspection Planning in Software Development Projects

In this article, we consider the problem of planning inspections and other tasks within a software development (SD) project with respect to the objectives quality (no. of defects), project duration, and costs. Based on a discrete-event simulation model of SD processes comprising the phases coding, inspection, test, and rework, we present a simplified formulation of the problem as a multiobjective optimization problem. For solving the problem (i. e. finding an approximation of the efficient set) we develop a multiobjective evolutionary algorithm. Details of the algorithm are discussed as well as results of its application to sample problems.
Key words: multiple objective programming, project management and scheduling, software development, evolutionary algorithms, efficient set
(29 pages, 2003)

43. T. Bortfeld , K.-H. Küfer, M. Monz, A. Scherrer, C. Thieke, H. Trinkaus

Intensity-Modulated Radiotherapy - A Large Scale Multi-Criteria Programming Problem -

Radiation therapy planning is always a tight rope walk between dangerous insufficient dose in the target volume and life threatening overdosing of organs at risk. Finding ideal balances between these inherently contradictory goals challenges dosimetrists and physicians in their daily practice. Today's planning systems are typically based on a single evaluation function that measures the quality of a radiation treatment plan. Unfortunately, such a one dimensional approach cannot satisfactorily map the different backgrounds of physicians and the patient dependent necessities. So, too often a time consuming iteration process between evaluation of dose distribution and redefinition of the evaluation function is needed.

In this paper we propose a generic multi-criteria approach based on Pareto's solution concept. For each entity of interest - target volume or organ at risk a structure dependent evaluation function is defined measuring deviations from ideal doses that are calculated from statistical functions. A reasonable bunch of clinically meaningful Pareto optimal solutions are stored in a data base, which can be interactively searched by physicians. The system guarantees dynamical planning as well as the discussion of tradeoffs between different entities.

Mathematically, we model the upcoming inverse problem as a multi-criteria linear programming problem. Because of the large scale nature of the problem it is not possible to solve the problem in a 3D-setting without adaptive reduction by appropriate approximation schemes.

Our approach is twofold: First, the discretization of the continuous problem is based on an adaptive hierarchical clustering process which is used for a local refinement of constraints during the optimization procedure. Second, the set of Pareto optimal solutions is approximated by an adaptive grid of representatives that are found by a hybrid process of calculating extreme compromises and interpolation methods.

Keywords: multiple criteria optimization, representative systems of Pareto solutions, adaptive triangulation, clustering and disaggregation techniques, visualization of Pareto solutions, medical physics, external beam radiotherapy planning, intensity modulated radiotherapy

(31 pages, 2003)

44. T. Halfmann, T. Wichmann

Overview of Symbolic Methods in Industrial Analog Circuit Design

Industrial analog circuits are usually designed using numerical simulation tools. To obtain a deeper circuit understanding, symbolic analysis techniques can additionally be applied. Approximation methods which reduce the complexity of symbolic expressions are needed in order to handle industrial-sized problems.

This paper will give an overview to the field of symbolic analog circuit analysis. Starting with a motivation, the state-of-the-art simplification algorithms for linear as well as for nonlinear circuits are presented. The basic ideas behind the different techniques are described, whereas the technical details can be found in the cited references. Finally, the application of linear and nonlinear symbolic analysis will be shown on two example circuits.

Keywords: CAD, automated analog circuit design, symbolic analysis, computer algebra, behavioral modeling, system simulation, circuit sizing, macro modeling, differential-algebraic equations, index

(17 pages, 2003)

45. S. E. Mikhailov, J. Orlik

Asymptotic Homogenisation in Strength and Fatigue Durability Analysis of Composites

Asymptotic homogenisation technique and two-scale convergence is used for analysis of macro-strength and fatigue durability of composites with a periodic structure under cyclic loading. The linear damage accumulation rule is employed in the phenomenological micro-durability conditions (for each component of the composite) under varying cyclic loading. Both local and non-local strength and durability conditions are analysed. The strong convergence of the strength and fatigue damage measure as the structure period tends to zero is proved and their limiting values are estimated.

Keywords: multiscale structures, asymptotic homogenization, strength, fatigue, singularity, non-local conditions

(14 pages, 2003)

46. P. Domínguez-Marín, P. Hansen, N. Mladenovi´c , S. Nickel

Heuristic Procedures for Solving the Discrete Ordered Median Problem

We present two heuristic methods for solving the Discrete Ordered Median Problem (DOMP), for which no such approaches have been developed so far. The DOMP generalizes classical discrete facility location problems, such as the p-median, p-center and Uncapacitated Facility Location problems. The first procedure proposed in this paper is based on a genetic algorithm developed by Moreno Vega [MV96] for p-median and p-center problems. Additionally, a second heuristic approach based on the Variable Neighborhood Search metaheuristic (VNS) proposed by Hansen & Mladenovic [HM97] for the p-median problem is described. An extensive numerical study is presented to show the efficiency of both heuristics and compare them.

Keywords: genetic algorithms, variable neighborhood search, discrete facility location

(31 pages, 2003)

47. N. Boland, P. Domínguez-Marín, S. Nickel, J. Puerto

Exact Procedures for Solving the Discrete Ordered Median Problem

The Discrete Ordered Median Problem (DOMP) generalizes classical discrete location problems, such as the N-median, N-center and Uncapacitated Facility Location problems. It was introduced by Nickel [16], who formulated it as both a nonlinear and a linear integer program. We propose an alternative integer linear programming formulation for the DOMP, discuss relationships between both integer linear programming formulations, and show how properties of optimal solutions can be used to strengthen these formulations. Moreover, we present a specific branch and bound procedure to solve the DOMP more efficiently. We test the integer linear programming formulations and this branch and bound method computationally on randomly generated test problems.

Keywords: discrete location, Integer programming

(41 pages, 2003)

48. S. Feldmann, P. Lang

Padé-like reduction of stable discrete linear systems preserving their stability

A new stability preserving model reduction algorithm for discrete linear SISO-systems based on their impulse response is proposed. Similar to the Padé approximation, an equation system for the Markov parameters involving the Hankel matrix is considered, that here however is chosen to be of very high dimension. Although this equation system therefore in general cannot be solved exactly, it is proved that the approximate solution, computed via the Moore-Penrose inverse, gives rise to a stability preserving reduction scheme, a property that cannot be guaranteed for the Padé approach. Furthermore, the proposed algorithm is compared to another stability preserving reduction approach, namely the balanced truncation method, showing comparable performance of the reduced systems. The balanced truncation method however starts from a state space description of the systems and in general is expected to be more computational demanding.

Keywords: Discrete linear systems, model reduction, stability, Hankel matrix, Stein equation

(16 pages, 2003)

49. J. Kallrath, S. Nickel

A Polynomial Case of the Batch Presorting Problem

This paper presents new theoretical results for a special case of the batch presorting problem (BPSP). We will show tht this case can be solved in polynomial time. Offline and online algorithms are presented for solving the BPSP. Competetive analysis is used for comparing the algorithms.

Keywords: batch presorting problem, online optimization, competetive analysis, polynomial algorithms, logistics

(17 pages, 2003)

50. T. Hanne, H. L. Trinkaus

knowCube for MCDM – Visual and Interactive Support for Multicriteria Decision Making

In this paper, we present a novel multicriteria decision support system (MCDSS), called knowCube, consisting of components for knowledge organization, generation, and navigation. Knowledge organization rests upon a database for managing qualitative and quantitative criteria, together with add-on information. Knowledge generation serves filling the database via e. g. identification, optimization, classification or simulation. For "finding needles in haycocks", the knowledge navigation component supports graphical database retrieval and interactive, goal-oriented problem solving. Navigation "helpers" are, for instance, cascading criteria aggregations, modifiable metrics, ergonomic interfaces, and customizable visualizations. Examples from real-life projects, e.g. in industrial engineering and in the life sciences, illustrate the application of our MCDSS.

Key words: Multicriteria decision making, knowledge management, decision support systems, visual interfaces, interactive navigation, real-life applications.

(26 pages, 2003)

51. O. Iliev, V. Laptev

On Numerical Simulation of Flow Through Oil Filters

This paper concerns numerical simulation of flow through oil filters. Oil filters consist of filter housing (filter box), and a porous filtering medium, which completely separates the inlet from the outlet. We discuss mathematical models, describing coupled flows in the pure liquid subregions and in the porous filter media, as well as interface conditions between them. Further, we reformulate the problem in fictitious regions method manner, and discuss peculiarities of the numerical algorithm in solving the coupled system. Next, we show numerical results, validating the model and the algorithm. Finally, we present results from simulation of 3-D oil flow through a real car filter.

Keywords: oil filters, coupled flow in plain and porous media, Navier-Stokes, Brinkman, numerical simulation

(8 pages, 2003)

52. W. Dörfler, O. Iliev, D. Stoyanov, D. Vassileva

On a Multigrid Adaptive Refinement Solver for Saturated Non-Newtonian Flow in Porous Media

A multigrid adaptive refinement algorithm for non-Newtonian flow in porous media is presented. The saturated flow of a non-Newtonian fluid is described by the continuity equation and the generalized Darcy law. The resulting second order nonlinear elliptic equation is discretized by a finite volume method on a cell-centered grid. A nonlinear full-multigrid, full-approximation-storage algorithm is implemented. As a smoother, a single grid solver based on Picard linearization and Gauss-Seidel relaxation is used. Further, a local refinement multigrid algorithm on a composite grid is developed. A residual based error indicator is used in the adaptive refinement criterion. A special implementation approach is used, which allows us to perform unstructured local refinement in conjunction with the finite volume discretization. Several results from numerical experiments are presented in order to examine the performance of the solver.

Keywords: Nonlinear multigrid, adaptive refinement, non-Newtonian flow in porous media

(17 pages, 2003)

53. S. Kruse

On the Pricing of Forward Starting Options under Stochastic Volatility

We consider the problem of pricing European forward starting options in the presence of stochastic volatility. By performing a change of measure using the asset

price at the time of strike determination as a numeraire, we derive a closed-form solution based on Heston's model of stochastic volatility.
Keywords: Option pricing, forward starting options, Heston model, stochastic volatility, cliquet options
(11 pages, 2003)

54. O. Iliev, D. Stoyanov

Multigrid – adaptive local refinement solver for incompressible flows

A non-linear multigrid solver for incompressible Navier-Stokes equations, exploiting finite volume discretization of the equations, is extended by adaptive local refinement. The multigrid is the outer iterative cycle, while the SIMPLE algorithm is used as a smoothing procedure. Error indicators are used to define the refinement subdomain. A special implementation approach is used, which allows to perform unstructured local refinement in conjunction with the finite volume discretization. The multigrid - adaptive local refinement algorithm is tested on 2D Poisson equation and further is applied to a lid-driven flows in a cavity (2D and 3D case), comparing the results with bench-mark data. The software design principles of the solver are also discussed.
Keywords: Navier-Stokes equations, incompressible flow, projection-type splitting, SIMPLE, multigrid methods, adaptive local refinement, lid-driven flow in a cavity
(37 pages, 2003)

55. V. Starikovicius

The multiphase flow and heat transfer in porous media

In first part of this work, summaries of traditional Multiphase Flow Model and more recent Multiphase Mixture Model are presented. Attention is being paid to attempts include various heterogeneous aspects into models. In second part, MMM based differential model for two-phase immiscible flow in porous media is considered. A numerical scheme based on the sequential solution procedure and control volume based finite difference schemes for the pressure and saturation-conservation equations is developed. A computer simulator is built, which exploits object-oriented programming techniques. Numerical result for several test problems are reported.
Keywords: Two-phase flow in porous media, various formulations, global pressure, multiphase mixture model, numerical simulation
(30 pages, 2003)

56. P. Lang, A. Sarishvili, A. Wirsen

Blocked neural networks for knowledge extraction in the software development process

One of the main goals of an organization developing software is to increase the quality of the software while at the same time to decrease the costs and the duration of the development process. To achieve this, various decisions e.ecting this goal before and during the development process have to be made by the managers. One appropriate tool for decision support are simulation models of the software life cycle, which also help to understand the dynamics of the software development process. Building up a simulation model requires a mathematical description of the interactions between di.erent objects involved in the development process. Based on experimental data, techniques from the .eld of knowledge discovery can be used to quantify these interactions and to generate new process knowledge based on the analysis of the determined relationships. In this paper blocked neuronal networks and related relevance measures will be presented as an appropriate tool for quanti.cation and validation of qualitatively known dependencies in the software development process.
Keywords: Blocked Neural Networks, Nonlinear Regression, Knowledge Extraction, Code Inspection
(21 pages, 2003)

57. H. Knaf, P. Lang, S. Zeiser

Diagnosis aiding in Regulation Thermography using Fuzzy Logic

The objective of the present article is to give an overview of an application of Fuzzy Logic in Regulation Thermography, a method of medical diagnosis support. An introduction to this method of the complementary medical science based on temperature measurements – so-called thermograms – is provided. The process of modelling the physician's thermogram evaluation rules using the calculus of Fuzzy Logic is explained.
Keywords: fuzzy logic,knowledge representation, expert system
(22 pages, 2003)

58. M.T. Melo, S. Nickel, F. Saldanha da Gama

Largescale models for dynamic multi-commodity capacitated facility location

In this paper we focus on the strategic design of supply chain networks. We propose a mathematical modeling framework that captures many practical aspects of network design problems simultaneously but which have not received adequate attention in the literature. The aspects considered include: dynamic planning horizon, generic supply chain network structure, external supply of materials, inventory opportunities for goods, distribution of commodities, facility configuration, availability of capital for investments, and storage limitations. Moreover, network configuration decisions concerning the gradual relocation of facilities over the planning horizon are considered. To cope with fluctuating demands, capacity expansion and reduction scenarios are also analyzed as well as modular capacity shifts. The relation of the proposed modeling framework with existing models is discussed. For problems of reasonable size we report on our computational experience with standard mathematical programming software. In particular, useful insights on the impact of various factors on network design decisions are provided.
Keywords: supply chain management, strategic planning, dynamic location, modeling
(40 pages, 2003)

59. J. Orlik

Homogenization for contact problems with periodically rough surfaces

We consider the contact of two elastic bodies with rough surfaces at the interface. The size of the micropeaks and valleys is very small compared with the macrosize of the bodies' domains. This makes the direct application of the FEM for the calculation of the contact problem prohibitively costly. A method is developed that allows deriving a macrocontact condition on the interface. The method involves the twoscale asymptotic homogenization procedure that takes into account the microgeometry of the interface layer and the stiffnesses of materials of both domains. The macrocontact condition can then be used in a FEM model for the contact problem on the macrolevel. The averaged contact stiffness obtained allows the replacement of the interface layer in the macromodel by the macrocontact condition.
Keywords: asymptotic homogenization, contact problems
(28 pages, 2004)

60. A. Scherrer, K.-H. Küfer, M. Monz, F. Alonso, T. Bortfeld

IMRT planning on adaptive volume structures – a significant advance of computational complexity

In intensity-modulated radiotherapy (IMRT) planning the oncologist faces the challenging task of finding a treatment plan that he considers to be an ideal compromise of the inherently contradictive goals of delivering a sufficiently high dose to the target while widely sparing critical structures. The search for this a priori unknown compromise typically requires the computation of several plans, i.e. the solution of several optimization problems. This accumulates to a high computational expense due to the large scale of these problems - a consequence of the discrete problem formulation. This paper presents the adaptive clustering method as a new algorithmic concept to overcome these difficulties. The computations are performed on an individually adapted structure of voxel clusters rather than on the original voxels leading to a decisively reduced computational complexity as numerical examples on real clinical data demonstrate. In contrast to many other similar concepts, the typical trade-off between a reduction in computational complexity and a loss in exactness can be avoided: the adaptive clustering method produces the optimum of the original problem. This flexible method can be applied to both single- and multi-criteria optimization methods based on most of the convex evaluation functions used in practice.
Keywords: Intensity-modulated radiation therapy (IMRT), inverse treatment planning, adaptive volume structures, hierarchical clustering, local refinement, adaptive clustering, convex programming, mesh generation, multi-grid methods
(24 pages, 2004)

61. D. Kehrwald

Parallel lattice Boltzmann simulation of complex flows

After a short introduction to the basic ideas of lattice Boltzmann methods and a brief description of a modern parallel computer, it is shown how lattice Boltzmann schemes are successfully applied for simulating fluid flow in microstructures and calculating material properties of porous media. It is explained how lattice Boltzmann schemes compute the gradient of the velocity field without numerical differentiation. This feature is then utilised for the simulation of pseudo-plastic fluids, and numerical results are presented for a simple benchmark problem as well as for the simulation of liquid composite moulding.
Keywords: Lattice Boltzmann methods, parallel computing, microstructure simulation, virtual material design, pseudo-plastic fluids, liquid composite moulding
(12 pages, 2004)

62. O. Iliev, J. Linn, M. Moog, D. Niedziela, V. Starikovicius

On the Performance of Certain Iterative Solvers for Coupled Systems Arising in Discretization of Non-Newtonian Flow Equations

Iterative solution of large scale systems arising after discretization and linearization of the unsteady non-Newtonian Navier–Stokes equations is studied. cross WLF model is used to account for the non-Newtonian behavior of the fluid. Finite volume method is used to discretize the governing system of PDEs. Viscosity is treated explicitely (e.g., it is taken from the previous time step), while other terms are treated implicitly. Different preconditioners (block–diagonal, block–triangular, relaxed incomplete LU factorization, etc.) are used in conjunction with advanced iterative methods, namely, BiCGStab, CGS, GMRES. The action of the preconditioner in fact requires inverting different blocks. For this purpose, in addition to preconditioned BiCGStab, CGS, GMRES, we use also algebraic multigrid method (AMG). The performance of the iterative solvers is studied with respect to the number of unknowns, characteristic velocity in the basic flow, time step, deviation from Newtonian behavior, etc. Results from numerical experiments are presented and discussed.
Keywords: Performance of iterative solvers, Preconditioners, Non-Newtonian flow
(17 pages, 2004)

63. R. Ciegis, O. Iliev, S. Rief, K. Steiner

On Modelling and Simulation of Different Regimes for Liquid Polymer Moulding

In this paper we consider numerical algorithms for solving a system of nonlinear PDEs arising in modeling of liquid polymer injection. We investigate the particular case when a porous preform is located within the mould, so that the liquid polymer flows through a porous medium during the filling stage. The nonlinearity of the governing system of PDEs is due to the non-Newtonian behavior of the polymer, as well as due to the moving free boundary. The latter is related to the penetration front and a Stefan type problem is formulated to account for it. A finite-volume method is used to approximate the given differential problem. Results of numerical experiments are presented.
We also solve an inverse problem and present algorithms for the determination of the absolute preform permeability coefficient in the case when the velocity of the penetration front is known from measurements. In both cases (direct and inverse problems) we emphasize on the specifics related to the non-Newtonian behavior of the polymer. For completeness, we discuss also the Newtonian case. Results of some experimental

measurements are presented and discussed.
Keywords: Liquid Polymer Moulding, Modelling, Simulation, Infiltration, Front Propagation, non-Newtonian flow in porous media
(43 pages, 2004)

64. T. Hanne, H. Neu

Simulating Human Resources in Software Development Processes

In this paper, we discuss approaches related to the explicit modeling of human beings in software development processes. While in most older simulation models of software development processes, esp. those of the system dynamics type, humans are only represented as a labor pool, more recent models of the discrete-event simulation type require representations of individual humans. In that case, particularities regarding the person become more relevant. These individual effects are either considered as stochastic variations of productivity, or an explanation is sought based on individual characteristics, such as skills for instance. In this paper, we explore such possibilities by recurring to some basic results in psychology, sociology, and labor science. Various specific models for representing human effects in software process simulation are discussed.
Keywords: Human resource modeling, software process, productivity, human factors, learning curve
(14 pages, 2004)

65. O. Iliev, A. Mikelic, P. Popov

Fluid structure interaction problems in deformable porous media: Toward permeability of deformable porous media

In this work the problem of fluid flow in deformable porous media is studied. First, the stationary fluid-structure interaction (FSI) problem is formulated in terms of incompressible Newtonian fluid and a linearized elastic solid. The flow is assumed to be characterized by very low Reynolds number and is described by the Stokes equations. The strains in the solid are small allowing for the solid to be described by the Lame equations, but no restrictions are applied on the magnitude of the displacements leading to strongly coupled, nonlinear fluid-structure problem. The FSI problem is then solved numerically by an iterative procedure which solves sequentially fluid and solid subproblems. Each of the two subproblems is discretized by finite elements and the fluid-structure coupling is reduced to an interface boundary condition. Several numerical examples are presented and the results from the numerical computations are used to perform permeability computations for different geometries.
Keywords: fluid-structure interaction, deformable porous media, upscaling, linear elasticity, stokes, finite elements
(28 pages, 2004)

66. F. Gaspar, O. Iliev, F. Lisbona, A. Naumovich, P. Vabishchevich

On numerical solution of 1-D poroelasticity equations in a multilayered domain

Finite volume discretization of Biot system of poroelasticity in a multilayered domain is presented. Staggered grid is used in order to avoid nonphysical oscillations of the numerical solution, appearing when a collocated grid is used. Various numerical experiments are presented in order to illustrate the accuracy of the finite difference scheme. In the first group of experiments, problems having analytical solutions are solved, and the order of convergence for the velocity, the pressure, the displacements, and the stresses is analyzed. In the second group of experiments numerical solution of real problems is presented.
Keywords: poroelasticity, multilayered material, finite volume discretization, MAC type grid
(41 pages, 2004)

67. J. Ohser, K. Schladitz, K. Koch, M. Nöthe

Diffraction by image processing and its application in materials science

A spectral theory for constituents of macroscopically homogeneous random microstructures modeled as homogeneous random closed sets is developed and provided with a sound mathematical basis, where the spectrum obtained by Fourier methods corresponds to the angular intensity distribution of x-rays scattered by this constituent. It is shown that the fast Fourier transform applied to three-dimensional images of microstructures obtained by micro-tomography is a powerful tool of image processing. The applicability of this technique is is demonstrated in the analysis of images of porous media.
Keywords: porous microstructure, image analysis, random set, fast Fourier transform, power spectrum, Bartlett spectrum
(13 pages, 2004)

68. H. Neunzert

Mathematics as a Technology: Challenges for the next 10 Years

No doubt: Mathematics has become a technology in its own right, maybe even a key technology. Technology may be defined as the application of science to the problems of commerce and industry. And science? Science maybe defined as developing, testing and improving models for the prediction of system behavior; the language used to describe these models is mathematics and mathematics provides methods to evaluate these models. Here we are! Why has mathematics become a technology only recently? Since it got a tool, a tool to evaluate complex, "near to reality" models: Computer! The model may be quite old – Navier-Stokes equations describe flow behavior rather well, but to solve these equations for realistic geometry and higher Reynolds numbers with sufficient precision is even for powerful parallel computing a real challenge. Make the models as simple as possible, as complex as necessary – and then evaluate them with the help of efficient and reliable algorithms: These are genuine mathematical tasks.
Keywords: applied mathematics, technology, modelling, simulation, visualization, optimization, glass processing, spinning processes, fiber-fluid interaction, trubulence effects, topological optimization, multicriteria optimization, Uncertainty and Risk, financial mathematics, Malliavin calculus, Monte-Carlo methods, virtual material design, filtration, bio-informatics, system biology
(29 pages, 2004)

69. R. Ewing, O. Iliev, R. Lazarov, A. Naumovich

On convergence of certain finite difference discretizations for 1D poroelasticity interface problems

Finite difference discretizations of 1D poroelasticity equations with discontinuous coefficients are analyzed. A recently suggested FD discretization of poroelasticity equations with constant coefficients on staggered grid, [5], is used as a basis. A careful treatment of the interfaces leads to harmonic averaging of the discontinuous coefficients. Here, convergence for the pressure and for the displacement is proven in certain norms for the scheme with harmonic averaging (HA). Order of convergence 1.5 is proven for arbitrary located interface, and second order convergence is proven for the case when the interface coincides with a grid node. Furthermore, following the ideas from [3], modified HA discretization are suggested for particular cases. The velocity and the stress are approximated with second order on the interface in this case. It is shown that for wide class of problems, the modified discretization provides better accuracy. Second order convergence for modified scheme is proven for the case when the interface coincides with a displacement grid node. Numerical experiments are presented in order to illustrate our considerations.
Keywords: poroelasticity, multilayered material, finite volume discretizations, MAC type grid, error estimates
(26 pages,2004)

70. W. Dörfler, O. Iliev, D. Stoyanov, D. Vassileva

On Efficient Simulation of Non-Newtonian Flow in Saturated Porous Media with a Multigrid Adaptive Refinement Solver

Flow of non-Newtonian in saturated porous media can be described by the continuity equation and the generalized Darcy law. Efficient solution of the resulting second order nonlinear elliptic equation is discussed here. The equation is discretized by a finite volume method on a cell-centered grid. Local adaptive refinement of the grid is introduced in order to reduce the number of unknowns. A special implementation approach is used, which allows us to perform unstructured local refinement in conjunction with the finite volume discretization. Two residual based error indicators are exploited in the adaptive refinement criterion. Second order accurate discretization on the interfaces between refined and non-refined subdomains, as well as on the boundaries with Dirichlet boundary condition, are presented here, as an essential part of the accurate and efficient algorithm. A nonlinear full approximation storage multigrid algorithm is developed especially for the above described composite (coarse plus locally refined) grid approach. In particular, second order approximation around interfaces is a result of a quadratic approximation of slave nodes in the multigrid - adaptive refinement (MG-AR) algorithm. Results from numerical solution of various academic and practice-induced problems are presented and the performance of the solver is discussed.
Keywords: Nonlinear multigrid, adaptive renement, non-Newtonian in porous media
(25 pages, 2004)

71. J. Kalcsics, S. Nickel, M. Schröder

Towards a Unified Territory Design Approach – Applications, Algorithms and GIS Integration

Territory design may be viewed as the problem of grouping small geographic areas into larger geographic clusters called territories in such a way that the latter are acceptable according to relevant planning criteria. In this paper we review the existing literature for applications of territory design problems and solution approaches for solving these types of problems. After identifying features common to all applications we introduce a basic territory design model and present in detail two approaches for solving this model: a classical location–allocation approach combined with optimal split resolution techniques and a newly developed computational geometry based method. We present computational results indicating the efficiency and suitability of the latter method for solving large–scale practical problems in an interactive environment. Furthermore, we discuss extensions to the basic model and its integration into Geographic Information Systems.
Keywords: territory desgin, political districting, sales territory alignment, optimization algorithms, Geographical Information Systems
(40 pages, 2005)

72. K. Schladitz, S. Peters, D. Reinel-Bitzer, A. Wiegmann, J. Ohser

Design of acoustic trim based on geometric modeling and flow simulation for non-woven

In order to optimize the acoustic properties of a stacked fiber non-woven, the microstructure of the non-woven is modeled by a macroscopically homogeneous random system of straight cylinders (tubes). That is, the fibers are modeled by a spatially stationary random system of lines (Poisson line process), dilated by a sphere. Pressing the non-woven causes anisotropy. In our model, this anisotropy is described by a one parametric distribution of the direction of the fibers. In the present application, the anisotropy parameter has to be estimated from 2d reflected light microscopic images of microsections of the non-woven.
After fitting the model, the flow is computed in digitized realizations of the stochastic geometric model using the lattice Boltzmann method. Based on the flow resistivity, the formulas of Delany and Bazley predict the frequency-dependent acoustic absorption of the non-woven in the impedance tube.
Using the geometric model, the description of a nonwoven with improved acoustic absorption properties is obtained in the following way: First, the fiber thicknesses, porosity and anisotropy of the fiber system are modified. Then the flow and acoustics simulations are performed in the new sample. These two steps are repeatedc for various sets of parameters. Finally, the set of parameters for the geometric model leading to the best acoustic absorption is chosen.
Keywords: random system of fibers, Poisson line process, flow resistivity, acoustic absorption, Lattice-Boltzmann method, non-woven
(21 pages, 2005)

73. V. Rutka, A. Wiegmann

Explicit Jump Immersed Interface Method for virtual material design of the effective elastic moduli of composite materials

Virtual material design is the microscopic variation of materials in the computer, followed by the numerical evaluation of the effect of this variation on the material's macroscopic properties. The goal of this procedure is an in some sense improved material. Here, we give examples regarding the dependence of the effective elastic moduli of a composite material on the geometry of the shape of an inclusion. A new approach on how to solve such interface problems avoids mesh generation and gives second order accurate results even in the vicinity of the interface.
The Explicit Jump Immersed Interface Method is a finite difference method for elliptic partial differential equations that works on an equidistant Cartesian grid in spite of non-grid aligned discontinuities in equation parameters and solution. Near discontinuities, the standard finite difference approximations are modified by adding correction terms that involve jumps in the function and its derivatives. This work derives the correction terms for two dimensional linear elasticity with piecewise constant coefficients, i. e. for composite materials. It demonstrates numerically convergence and approximation properties of the method.
Keywords: virtual material design, explicit jump immersed interface method, effective elastic moduli, composite materials
(22 pages, 2005)

74. T. Hanne

Eine Übersicht zum Scheduling von Baustellen

Im diesem Dokument werden Aspekte der formalen zeitlichen Planung bzw. des Scheduling für Bauprojekte anhand ausgewählter Literatur diskutiert. Auf allgemeine Aspekte des Scheduling soll dabei nicht eingegangen werden. Hierzu seien als Standard-Referenzen nur Brucker (2004) und Pinedo (1995) genannt. Zu allgemeinen Fragen des Projekt-Managements sei auf Kerzner (2003) verwiesen.
Im Abschnitt 1 werden einige Anforderungen und Besonderheiten der Planung von Baustellen diskutiert. Diese treten allerdings auch in zahlreichen anderen Bereichen der Produktionsplanung und des Projektmanagements auf. In Abschnitt 2 werden dann Aspekte zur Formalisierung von Scheduling-Problemen in der Bauwirtschaft diskutiert, insbesondere Ziele und zu berücksichtigende Restriktionen. Auf eine mathematische Formalisierung wird dabei allerdings verzichtet. Abschnitt 3 bietet eine Übersicht über Verfahren und grundlegende Techniken für die Berechnung von Schedules. In Abschnitt 4 wird ein Überblick über vorhandene Software, zum einen verbreitete Internationale Software, zum anderen deutschsprachige Branchenlösungen, gegeben. Anschließend werden Schlussfolgerungen gezogen und es erfolgt eine Auflistung der Literaturquellen.
Keywords: Projektplanung, Scheduling, Bauplanung, Bauindustrie
(32 pages, 2005)

75. J. Linn

The Folgar–Tucker Model as a Differential Algebraic System for Fiber Orientation Calculation

The Folgar–Tucker equation (FTE) is the model most frequently used for the prediction of fiber orientation (FO) in simulations of the injection molding process for short–fiber reinforced thermoplasts. In contrast to its widespread use in injection molding simulations, little is known about the mathematical properties of the FTE: an investigation of e. g. its phase space M_{FT} has been presented only recently [12]. The restriction of the dependent variable of the FTE to the set M_{FT} turns the FTE into a differential algebraic system (DAS), a fact which is commonly neglected when devising numerical schemes for the integration of the FTE. In this article we present some recent results on the problem of trace stability as well as some introductory material which complements our recent paper [12].
Keywords: fiber orientation, Folgar–Tucker model, invariants, algebraic constraints, phase space, trace stability
(15 pages, 2005)

76. M. Speckert, K. Dreßler, H. Mauch, A. Lion, G. J. Wierda

Simulation eines neuartigen Prüfsystems für Achserprobungen durch MKS-Modellierung einschließlich Regelung

Testing new suspensions based on real load data is performed on elaborate multi channel test rigs. Usually, wheel forces and moments measured during driving maneuvers are reproduced by the test rig. Because of the complicated interaction between test rig and suspension each new rig configuration has to prove its efficiency with respect to the requirements and the configuration might be subject to optimization.
This paper deals with mathematical and physical modeling of a new concept of a test rig which is based on two hexapods. The model contains the geometric configuration as well as the hydraulics and the controller. It is implemented as an ADAMS/Car template and can be combined with different suspension models to get a complete assembly representing the entire test rig. Using this model, all steps required for a real test run such as controller adaptation, drive file iteration and simulation can be performed. Geometric or hydraulic parameters can be modified easily to improve the setup and adapt the system to the suspension and the given load data.
The model supports and accompanies the introduction of the new rig concept and can be used to prepare real tests on a virtual basis. Using both a front and a rear suspension the approach is described and the potentials coming with the simulation are pointed out.
Keywords: virtual test rig, suspension testing, multibody simulation, modeling hexapod test rig, optimization of test rig configuration
(20 pages, 2005)
In deutscher Sprache; bereits erschienen in: VDI-Berichte Nr. 1900, VDI-Verlag GmbH Düsseldorf (2005), Seiten 227-246

77. K.-H. Küfer, M. Monz, A. Scherrer, P. Süss, F. Alonso, A. S. A. Sultan, Th. Bortfeld, D. Craft, Chr. Thieke

Multicriteria optimization in intensity modulated radiotherapy planning

Inverse treatment planning of intensity modulated radiothrapy is a multicriteria optimization problem: planners have to find optimal compromises between a sufficiently highdose intumor tissuethat garantuee a high tumor control, and, dangerous overdosing of critical structures, in order to avoid high normal tissue complcication problems.
The approach presented in this work demonstrates how to state a flexible generic multicriteria model of the IMRT planning problem and how to produce clinically highly relevant Pareto-solutions. The model is imbedded in a principal concept of Reverse Engineering, a general optimization paradigm for design problems. Relevant parts of the Pareto-set are approximated by using extreme compromises as cornerstone solutions, a concept that is always feasible if box constraints for objective funtions are available. A major practical drawback of generic multicriteria concepts trying to compute or approximate parts of the Pareto-set is the high computational effort. This problem can be overcome by exploitation of an inherent asymmetry of the IMRT planning problem and an adaptive approximation scheme for optimal solutions based on an adaptive clustering preprocessing technique. Finally, a coherent approach for calculating and selecting solutions in a real-timeinteractive decision-making process is presented. The paper is concluded with clinical examples and a discussion of ongoing research topics.
Keywords: multicriteria optimization, extreme solutions, real-time decision making, adaptive approximation schemes, clustering methods, IMRT planning, reverse engineering
(51 pages, 2005)

78. S. Amstutz, H. Andrä

A new algorithm for topology optimization using a level-set method

The levelset method has been recently introduced in the field of shape optimization, enabling a smooth representation of the boundaries on a fixed mesh and therefore leading to fast numerical algorithms. However, most of these algorithms use a HamiltonJacobi equation to connect the evolution of the levelset function with the deformation of the contours, and consequently they cannot create any new holes in the domain (at least in 2D). In this work, we propose an evolution equation for the levelset function based on a generalization of the concept of topological gradient. This results in a new algorithm allowing for all kinds of topology changes.
Keywords: shape optimization, topology optimization, topological sensitivity, level-set
(22 pages, 2005)

79. N. Ettrich

Generation of surface elevation models for urban drainage simulation

Traditional methods fail for the purpose of simulating the complete flow process in urban areas as a consequence of heavy rainfall and as required by the European Standard EN-752 since the bi-directional coupling between sewer and surface is not properly handled. The methodology, developed in the BMBF/EUREKA-project RisUrSim, solves this problem by carrying out the runoff on the basis of shallow water equations solved on high-resolution surface grids. Exchange nodes between the sewer and the surface, like inlets and manholes, are located in the computational grid and water leaving the sewer in case of surcharge is further distributed on the surface.
So far, it has been a problem to get the dense topographical information needed to build models suitable for hydrodynamic runoff calculation in urban areas. Recent airborne data collection methods like laser scanning, however, offer a great chance to economically gather densely sampled input data. This paper studies the potential of such laser-scan data sets for urban water hydrodynamics.
Keywords: Flooding, simulation, urban elevation models, laser scanning
(22 pages, 2005)

80. H. Andrä, J. Linn, I. Matei, I. Shklyar, K. Steiner, E. Teichmann

OPTCAST – Entwicklung adäquater Strukturoptimierungsverfahren für Gießereien Technischer Bericht (KURZFASSUNG)

Im vorliegenden Bericht werden die Erfahrungen und Ergebnisse aus dem Projekt **OptCast** zusammengestellt. Das Ziel dieses Projekts bestand (a) in der Anpassung der Methodik der automatischen Strukturoptimierung für Gussteile und (b) in der Entwicklung und Bereitstellung von gießereispezifischen Optimierungstools für Gießereien und Ingenieurbüros.
Gießtechnische Restriktionen lassen sich nicht auf geometrische Restriktionen reduzieren, sondern sind nur über eine Gießsimulation (Erstarrungssimulation und Eigenspannungsanalyse) adäquat erfassbar, da die lokalen Materialeigenschaften des Gussteils nicht nur von der geometrischen Form des Teils, sondern auch vom verwendeten Material abhängen. Wegen dieser Erkenntnis wurde ein neuartiges iteratives Topologieoptimierungsverfahren unter Verwendung der Level-Set-Technik entwickelt, bei dem keine variable Dichte des Materials eingeführt wird. In jeder Iteration wird ein scharfer Rand des Bauteils berechnet. Somit ist die Gießsimulation in den iterativen Optimierungsprozess integrierbar.
Der Bericht ist wie folgt aufgebaut: In Abschnitt 2 wird der Anforderungskatalog erläutert, der sich aus der Bearbeitung von Benchmark-Problemen in der ersten Projektphase ergab. In Abschnitt 3 werden die Benchmark-Probleme und deren Lösung mit den im Projekt entwickelten Tools beschrieben. Abschnitt 4 enthält die Beschreibung der neu entwickelten Schnittstellen und die mathematische Formulierung des Topologieoptimierungsproblems. Im letzten Abschnitt wird das neue Topologieoptimierungsverfahren, das die Simulation des Gießprozesses einschließt, erläutert.
Keywords: Topologieoptimierung, Level-Set-Methode, Gießprozesssimulation, Gießtechnische Restriktionen, CAE-Kette zur Strukturoptimierung
(77 pages, 2005)

81. N. Marheineke, R. Wegener

Fiber Dynamics in Turbulent Flows Part I: General Modeling Framework

The paper at hand deals with the modeling of turbulence effects on the dynamics of a long slender elastic fiber. Independent of the choice of the drag model, a general aerodynamic force concept is derived on the basis of the velocity field for the randomly fluctuating component of the flow. Its construction as centered differentiable Gaussian field complies thereby with the requirements of the stochastic k-ε turbulence model and Kolmogorov's universal equilibrium theory on local isotropy.

Keywords: fiber-fluid interaction; Cosserat rod; turbulence modeling; Kolmogorov's energy spectrum; double-velocity correlations; differentiable Gaussian fields

Part II: Specific Taylor Drag

In [12], an aerodynamic force concept for a general air drag model is derived on top of a stochastic k-ε description for a turbulent flow field. The turbulence effects on the dynamics of a long slender elastic fiber are particularly modeled by a correlated random Gaussian force and in its asymptotic limit on a macroscopic fiber scale by Gaussian white noise with flow-dependent amplitude. The paper at hand now presents quantitative similarity estimates and numerical comparisons for the concrete choice of a Taylor drag model in a given application.

Keywords: flexible fibers; k-ε turbulence model; fiber-turbulence interaction scales; air drag; random Gaussian aerodynamic force; white noise; stochastic differential equations; ARMA process

(38 pages, 2005)

82. C. H. Lampert, O. Wirjadi

An Optimal Non-Orthogonal Separation of the Anisotropic Gaussian Convolution Filter

We give ananalytical and geometrical treatment of what it means to separate a Gaussian kernel along arbitrary axes in R^n, and we present a separation scheme that allows to efficiently implement anisotropic Gaussian convolution filters in arbitrary dimension. Based on our previous analysis we show that this scheme is optimal with regard to the number of memory accesses and interpolation operations needed.

Our method relies on non-orthogonal convolution axes and works completely in image space. Thus, it avoids the need for an FFT-subroutine. Depending on the accuracy and speed requirements, different interpolation schemes and methods to implement the one-dimensional Gaussian (FIR, IIR) can be integrated. The algorithm is also feasible for hardware that does not contain a floating-point unit.

Special emphasis is laid on analyzing the performance and accuracy of our method. In particular, we show that without anyspecial optimization of the source code, our method can perform anisotropic Gaussian filtering faster than methods relying on the Fast Fourier Transform.

Keywords: Anisotropic Gaussian filter, linear filtering, orientation space, nD image processing, separable filters

(25 pages, 2005)

83. H. Andrä, D. Stoyanov

Error indicators in the parallel finite element solver for linear elasticity DDFEM

This report discusses two approaches for a posteriori error indication in the linear elasticity solver DDFEM: An indicator based on the Richardson extrapolation and Zienkiewicz-Zhu-type indicator.

The solver handles 3D linear elasticity steady-state problems. It uses own input language to de-scribe the mesh and the boundary conditions. Finite element discretization over tetrahedral meshes with first or second order shape functions (hierarchical basis) has been used to resolve the model. The parallelization of the numerical method is based on the domain decomposition approach. DDFEM is highly portable over a set of parallel computer architectures supporting the MPI-standard.

Keywords: linear elasticity, finite element method, hierarchical shape functions, domain decom-position, parallel implementation, a posteriori error estimates

(21 pages, 2006)

84. M. Schröder, I. Solchenbach

Optimization of Transfer Quality in Regional Public Transit

In this paper we address the improvement of transfer quality in public mass transit networks. Generally there are several transit operators offering service and our work is motivated by the question how their timetables can be altered to yield optimized transfer possibilities in the over-all network. To achieve this, only small changes to the timetables are allowed.

The set-up makes it possible to use a quadratic semi-assignment model to solve the optimization problem. We apply this model, equipped with a new way to assess transfer quality, to the solu-tion of four real-world examples. It turns out that improvements in overall transfer quality can be determined by such optimization-based techniques. Therefore they can serve as a first step to-wards a decision support tool for planners of regional transit networks.

Keywords: public transit, transfer quality, quadratic assignment problem

(16 pages, 2006)

85. A. Naumovich, F. J. Gaspar

On a multigrid solver for the three-dimensional Biot poroelasticity system in multilayered domains

In this paper, we present problem-dependent prolongation and problem-dependent restriction for a multigrid solver for the three-dimensional Biot poroelasticity system, which is solved in a multilayered domain. The system is discretized on a staggered grid using the finite volume method. During the discretization, special care is taken of the discontinuous coefficients. For the efficient multigrid solver, a need in operator-dependent restriction and/or prolongation arises. We derive these operators so that they are consistent with the discretization. They account for the discontinuities of the coefficients, as well as for the coupling of the unknowns within the Biot system. A set of numerical experiments shows necessity of use of the operator-dependent restriction and prolongation in the multigrid solver for the considered class of problems.

Keywords: poroelasticity, interface problem, multigrid, operator-dependent prolongation

(11 pages, 2006)

86. S. Panda, R. Wegener, N. Marheineke

Slender Body Theory for the Dynamics of Curved Viscous Fibers

The paper at hand presents a slender body theory for the dynamics of a curved inertial viscous Newtonian fiber. Neglecting surface tension and temperature dependence, the fiber flow is modeled as a three-dimensional free boundary value problem via instationary incompressible Navier-Stokes equations. From regular asymptotic expansions in powers of the slenderness parameter leading-order balance laws for mass (cross-section) and momentum are derived that combine the unrestricted motion of the fiber center-line with the inner viscous transport. The physically reasonable form of the one-dimensional fiber model results thereby from the introduction of the intrinsic velocity that characterizes the convective terms.

Keywords: curved viscous fibers; fluid dynamics; Navier-Stokes equations; free boundary value problem; asymptotic expansions; slender body theory

(14 pages, 2006)

Status quo: March 2006